Nfkbid **is required for immunity and antibody responses to** ***Toxoplasma gondii***

Scott P Souza[1], Samantha D Splitt[1], Julia A Alvarez[1], Jessica N Wilson[1], Safuwra Wizzard[1], Zheng Luo[3], Nicole Baumgarth[3], Kirk DC Jensen[1, 2#]

[1]School of Natural Sciences, University of California, Merced

[2]Health Science Research Institute, University of California, Merced

[3]Center for Immunology & Infectious Diseases, and Department of Pathology, Microbiology and Immunology, University of California, Davis

Correspondence: Kirk D.C. Jensen, kjensen5@ucmerced.edu

Abstract

Protective humoral responses are important in generating natural immunity to parasitic infections but have been difficult to elicit by vaccines. Among parasites that evade vaccine-induced immunity is *Toxoplasma gondii*. We previously reported that South American strains of *Toxoplasma gondii* are adept at immune evasion and cause lethal secondary infections in chronically infected mice. Here we report that unlike susceptible C57BL/6J mice, A/J mice were highly resistant to secondary infection. To identify correlates of immunity, mouse genetics were used to map immunity loci that segregated within a recombinant inbred panel (AxB, BxA). We identified *Nfkbid*, a nuclear regulator of NF-κB that is required for B cell activation and B-1 cell development. *Nfkbid*-null mice (bumble) were susceptible to secondary, but not primary infections. Bumble mice did not generate

parasite-specific IgM and lacked robust parasite-specific IgG, which correlated with defects in B-2 cell maturation and class-switch recombination. Though high-affinity antibodies are B-2 derived, B-1 cells are absent in bumble mice and transfer of B-1 cells partially rescued the observed immunity defect. In comparison, humoral immunity to *T. gondii* in resistant A/J mice correlated with robust isotype class-switching in both B cell lineages, which can be fine-tuned by *Nfkbid* gene expression. We propose a model where humoral immunity to *T. gondii* is driven by *Nfkbid* and must be 'layered' by both B-1 and B-2 cells to promote protection to virulent challenge.

Significance Statement

Eukaryotic parasitic diseases account for approximately one fifth of all childhood deaths, yet no highly protective vaccine exists for any human parasite. More research must be done to discover how to elicit protective vaccine-induced immunity to parasitic pathogens. We used an unbiased genetic screen to find key genes responsible for immunity to the eukaryotic parasite *Toxoplasma gondii*. Our screen found *Nfkbid* a transcription factor that controls B cell development and activation. Mice without *Nfkbid* were highly susceptible to *T. gondii* and were deficient at making antibodies against the parasite. *Nfkbid* and other peaks identified in our unbiased screen represent potential targets for vaccines to elicit protective immune responses against parasitic pathogens.

Main Text

Introduction

The goal of vaccination is to induce immunological memory that can protect from natural infection challenge. Depending on the pathogen, effective memory would need to protect

also against a wide variety of pathogen-specific strains encountered in nature. Such protection is termed heterologous immunity, and is effective against pathogen strains that differ in virulence, immune evasion or polymorphic antigens. Parasites represent a special challenge to vaccine development. Indeed, an entirely protective vaccine has yet to be achieved for any human parasite (1). The apicomplexan parasite *Toxoplasmas gondii*, provides an excellent system to explore requirements for heterologous immunity to a parasitic pathogen. *T. gondii* is a globally spread intracellular protozoan parasite of warm-blooded animals that exhibits great genetic diversity (2). *T. gondii* strains differ dramatically in primary infection virulence in laboratory mice (3) and in severity of human toxoplasmosis (4-7). Such infections can be overcome by immunological memory responses elicited by vaccination or natural infection. In particular, memory CD8 T cells and induction of IFNγ are primarily responsible for protection against lethal secondary infections with the widely studied type I RH strain, which has a lethal dose of one parasite in naïve mice (8-13). CD4 T cells are required to help the formation of effector CD8 T cell (14, 15) and B cell responses (16), but the ability to adoptively transfer vaccine-elicited cellular immunity to naïve recipients against the type I RH challenge is unique to memory CD8 T cells (10, 11).

The role of B cells in *T. gondii* infections is less understood. Previous studies showed that B cell deficient mice (muMT) are extremely susceptible to primary (17), chronic (18) and secondary infections (19), despite unimpaired levels of IFNγ. Passive transfer of antibodies from immunized animals into vaccinated muMT mice significantly prolongs their survival after challenge (16, 19). IgM seems particularly suited for blocking cellular invasion by *T. gondii* (20), while IgG can perform both neutralization (21) and opsonization functions (22-24). Antibody responses against *T. gondii* are dependent on CD4 T cells (16, 25), and are regulated by cytokines that modulate T follicular helper cell

and germinal center B cell formation in secondary lymphoid organs (26, 27), suggesting conventional “B-2” B cell responses provide antibody-mediated immunity to *T. gondii.*

In addition, “B-1” cells are innate-like lymphocytes that are known for producing self- and pathogen-reactive “natural” IgM. B-1 cells are the predominant B cell compartment within the body cavities, including the peritoneal and pleural spaces and contribute to antigen-specific responses to many pathogens (reviewed in (28)). In mouse models of secondary bacterial infections, including *Borrelia hermsii* (29), *Streptococcus pneumoniae* (30) and non-typhoid *Salmonella* (31), vaccination induces protective memory B-1 cells to T cell-independent bacterial antigens. This memory is often restricted to the B-1(b), or CD5- subset of B-1 cells (32), but not in all models (33). In the *T. gondii* model, one study suggested that primed CD5+ B-1(a) cells can rescue B-cell-deficient mice during primary infection with a low virulence strain (17). Memory B cells are also appreciated to secrete pathogen-specific IgM (34), and generate somatically mutated IgM to combat blood stage secondary infection with *Plasmodium* (35). Whether IgM responses to *T. gondii* are B-2 or B-1 derived is unknown. Moreover, the role of B-1 cells in promoting immunity to *T. gondii* during a secondary infection has yet to be determined.

Particularly troubling for vaccine development for *T. gondii* is the lack of sterilizing immunity achieved following infection (36, 37). Unlike the highly passaged lab type I RH strain, for which most immunological memory studies have been performed, the less passaged type I GT1 strain and atypical strains, many of which are endemic to South America, cause lethal secondary infections in C57BL/6J mice and co-infect (i.e. ‘superinfect’) the brains of challenged survivors (37). During secondary infection memory CD8 T cells become exhausted, but checkpoint blockade fails to reverse disease outcome (38). The data suggest yet unknown mechanisms are needed to provide heterologous immunity to highly virulent strains of *T. gondii*. Therefore, we set out to address whether

additional requirements are necessary for heterologous immunity to *T. gondii*. Through use of forward and reverse genetics, we discovered a previously unidentified, essential role for *Nfkbid* in immunity and antibody responses to *T. gondii*, and present evidence that both B-1 and B-2 cells may assist effective immunity to secondary infection with highly virulent parasite strains.

Results

Non-MHC loci control resistance to secondary infection with *Toxoplasma gondii*

When mice are given a natural infection with a low virulent type III CEP strain and allowed to progress to chronic infection for 35-42 days, the immunological memory that develops is known to protect against secondary infections with the commonly studied lab strain, type I RH. In contrast, highly virulent "atypical" strains such as those isolated from South America (VAND, GUYDOS, GUYMAT, TgCATBr5) or France (MAS, GPHT, FOU) and the clonal type I GT1 strain led to morbidity and mortality in C57BL/6J mice at varying frequencies, depending on the strain type and their virulence factors (37). To explore whether host genetics influenced the ability to survive secondary infection, a similar experiment was performed with A/J mice. In contrast to C57BL/6 mice, A/J mice were resistant to secondary infection with all virulent atypical *T. gondii* strains analyzed (Fig 1A) and cleared parasite burden as early as day 4 post challenge (Fig 1B). In contrast, naïve A/J mice succumb to infection (not shown), consistent with the known susceptibility of laboratory mice to type I and atypical strain infections (37, 39, 40). These results suggest that at least one or more genetic loci controls immunity to secondary infection with *T. gondii* strains.

A/J mice are known to be resistant to primary infections with the intermediate virulent type II strain (41, 42), and prevent cyst formation due to polymorphisms in their

MHC class I H-2 molecule, L^d (43, 44). To determine the extent to which the H-2a locus may contribute to A/J mice's resistance to secondary infection we compared infections in C57BL/10 (B10) and C57BL/10.A (B10.A) mouse strains, the latter carrying the MHC H-2 locus of A/J (H-2a) in place of C57BL/6's MHC H-2 (H-2b). Compared to mice with the H-2b haplotype, mice expressing H-2a had less cysts and weighed more during chronic infection with type III strains ($P<0.04$; Fig S1). Despite their relative health at the time of challenge, B10.A mice were highly susceptible (0%-30% survival) to secondary infection with certain atypical strains (VAND, GUY-DOS, GPHT, FOU), but displayed varying degrees of resistance to others (TgCATBr5, MAS, GUY-MAT; 60-100% survival) (Fig 1A). In the case of MAS secondary infection, B10.A mice but not B10 mice were highly resistant and exhibited reduced parasite burden by day 8 post challenge (Fig 1B). Together, the data suggest that while the MHC H-2a locus is an important modifier of resistance to certain *T. gondii* strains, this is not true for every challenge. Importantly, the A/J genetic background encodes additional non-MHC-linked genes that control immunity to *T. gondii*.

Genetic mapping reveals four loci that correlate with immunity to *Toxoplasma gondii*

To identify non-MHC loci that promote resistance to secondary infection, we first analyzed the outcome of infection with the type I GT1 *T. gondii* strain, as this strain caused lethal secondary infections in B10 and B10.A, but not in A/J or first filial generation A/J x C57BL/6J mice ('F1') (Fig 1C). Following secondary infections, A/J and F1 mice showed no overt symptoms of weight loss, dehydration, or lethargy (not shown). However, sterile immunity was not achieved. For example, the GT1 strain was present in the brains of these survivors (i.e. 'superinfection'), and at greater frequencies in F1 compared to A/J mice (Fig 1D). Superinfections were also detected at high frequencies in B10 and B10.A

surviving mice challenged with atypical strains. Overall, mice of the C57BL genetic background were more prone to superinfection compared to A/J mice (Table S1). It is unknown whether virulent strains of *T. gondii* have evolved to superinfect hosts with immunological memory, as previously hypothesized (37). Nonetheless, our results underscore the difficulty in achieving sterile immunity to parasites in otherwise genetically 'resistant' hosts.

Then we performed secondary infection experiments with the type I GT1 strain using 26 recombinant inbred (RI) mice (Table S2). The AxB:BxA RI mouse panel contains an assortment of homozygous A/J and C57BL/6 alleles, which assist genetic mapping of loci that contribute to various phenotypes, including those related to *T. gondii* infection (41, 45, 46). Genetic mapping revealed four distinct Quantitative Trait Loci (QTL) peaks with logarithm of the odds (LOD) scores greater than 3 on chromosomes 7, 10, 11 and 17 (Fig 2A). None of the QTLs bore evidence for epistatic interactions (not shown), and only the chromosome 10 QTL surpassed genome-wide permutation testing (n=1000, $P<0.05$). Nevertheless, an additive-QTL model including all four QTLs best fit the data compared to any lesser combination of them ($P<0.02$, ANOVA). The estimated effect on the phenotypic variance observed in the RI panel is 24%, 41%, 21% and 27% for the chromosome (chr) 7, 10, 11 and 17 QTLs, respectively. Consistent with these estimates, complete phenotypic penetrance (i.e. allelic correlation at 100%) was not observed for any locus (Fig 2B). Moreover, replacing chromosomes 7 or 10 of C57BL/6J with those of A/J conferred no survival advantage to secondary infection in consomic mice (Fig S2). Regardless, small effect QTLs controlling complex traits can still lead to the identification of causal genes within a QTL region, as occurred for the successful identification of MHC 1 L^d as the host resistance factor to chronic *T. gondii* infection (43).

Nfkbid is one of the most polymorphic genes within the chr7 QTL region (Mb 30.3-33.0) and sits between the genetic markers that flank the highest imputed LOD score (Table S3). This gene encodes IκBNS, which is a member of atypical NF-κB inhibitors, called nuclear IκBs, reflecting their restricted cellular localization. Unlike classical inhibitors of NF-κB, atypical NF-κB inhibitors can modulate NF-κB to induce or repress transcription (47). Previous work has shown that *Nfkbid* null mice completely fail to develop B-1 cells (48, 49), lack circulating IgM and IgG3 antibodies, and cannot respond to T-independent (T-I) type II antigens such as NP-ficoll (48-50). IκBNS also promotes B-2 cell activation and isotype class switching (48), enhances T cell production of IL-2 and IFNγ (51), supports development of T regulatory cells (52) and suppresses TLR-induced cytokine expression in macrophages (53). The tetraspanin, *Tspan8,* is within the chr10 QTL (Mb 115.8-116.2) and is the most highly polymorphic gene between A/J and C57BL/6J mice in this region (Table S3). *Tspan8* is 6-fold more highly expressed in spleens from A/J compared to C57BL/6 mice (immgen.org). *Tspan8* promotes cancer metastasis (54) and can impact leukocyte migration (55), but its role in immunity is largely unknown. Other polymorphic gene candidates within the four QTLs are listed in Table S3.

***Nfkbid* on chromosome 7 is required for immunity and the generation of *Toxoplasma gondii*-specific antibodies**

Given the role of *Nfkbid* in several immune functions, degree of polymorphism and central location within the chr7 QTL, the requirement for *Nfkbid* in immunity to *T. gondii* was further explored. *Nfkbid* null “bumble” mice (C57BL/6J) have previously been described, which were derived from an ENU mutagenesis screen. These mice possess a premature stop codon in *Nfkbid,* rendering them unable to support T-I antibody responses and B-1 development (49). Bumble mice survived primary infection with the low virulent

CEP strain at frequencies similar to wildtype C57BL/6J mice (Fig 2C) but succumbed to secondary infection three days earlier when challenged with the GT1 strain (Fig 2D). Since the C57BL genetic background is uniformly susceptible to GT1 secondary infections used in our genetic screen, susceptibility to challenge with the commonly studied type I RH strain was explored, which is normally controlled in vaccinated or chronically infected mice (8-13). Importantly, bumble mice were entirely susceptible to secondary infection with the type I RH strain (Fig 2E), which exhibited greater parasite loads compared to wildtype mice (Fig 2F). Moreover, bumble mice failed to generate parasite specific-IgM, and were poor producers of parasite-specific IgG3, IgG2b and IgG2a antibody responses after chronic infection (Fig 3A). The remaining antibodies that were secreted exhibited defects in their ability to block parasite invasion of host cells (Fig 3B). Antibodies from naïve mice fail to bind *T. gondii*, thus natural antibodies do not recognize *T. gondii,* consistent with previous reports (20). Although *Nfkbid* promotes T cell production of IFNγ and IL-2 in in vitro stimulation assays (51) and promotes thymic development of FOXP3+ T regulatory cells (52), no impairment of T cell cytokine production was observed, nor were frequencies of FOXP3+ CD25^{hi} CD4+ T regulatory cells altered in bumble compared to wildtype mice during secondary infection (Fig S3).

To determine where the breakdown in the B cell response occurred in bumble mice, immunophenotyping was employed. Consistent with previous reports, bumble mice have greatly reduced marginal zone B cells in naïve mice and did not increase in frequency during *T. gondii* infection (not shown). Atypical B cells (FCLR5+ CD80+ CD73+) which respond to *Plasmodium* infections in mice (56) were also reduced in bumble compared to B6 mice following *T. gondii* infection (not shown). The memory CD73+ B cell compartment in bumble mice bore evidence for reduced class switching during *T. gondii* infection, as

they remain mainly IgM+IgD+ while C57BL/6J mice have higher frequencies of IgM-IgD- cells (Fig 3C). Most pronounced, however, is a large accumulation of transitional stage immature B-2 cells in bumble mice that occurs during chronic infection, implicating that B cell responses to *T. gondii* may require reinforcement from recent bone marrow derived emigrants and that this previously hidden mobilization is blocked in the absence of *Nfkbid*. Hence, *Nfkbid* is not only an important regulator of B-1 cell development through the transitional stage of immature B cell development in the steady state (57), but also for B-2 cell maturation, differentiation and activation during *T. gondii* infection.

Defective B-2 responses underlie bumble's defect in humoral immunity

The impaired ability of bumble mice to generate parasite-specific antibodies, combined with the documented collapse of the B-1 cell compartment in *Nfkbid*-deficient mice (48, 49), prompted us to directly assess the role of B-1 mediated immunity and humoral responses to *T. gondii*. First, total peritoneal exudate cells (PerC) were adoptively transferred into bumble mice at day 2 of birth, which allows optimal B-1 engraftment and self-renew for the life of the animal (58). Then, bumble mice that received total PerC transfers were infected with the avirulent type III strain at 6-7 weeks of age and given a secondary infection 35 days later with the type I RH strain (Fig 4A). Bumble mice receiving PerC partially reconstituted serum IgM to ~40% of wildtype levels (Fig S4), consistent with previous studies (58), and had a significantly delayed time to death relative to non-transferred littermates following type I RH challenge (Fig 4A). Previous studies have shown B-1 cells respond to infections and create both pathogen- (29, 30, 32, 59) and microbiota -specific antibodies (60). Antibody profiling of bumble mice that received PerC transfer showed a trend of increased anti-*T. gondii* antibody generation following chronic infection (Fig 4B), but antibody reactivity to the parasite did not reach levels observed in

wildtype mice, suggesting the B-1 compartment has a limited role in generating high-affinity parasite-specific antibodies. The B cell compartment responsible for generating parasite-specific antibody was further confirmed with Igh-allotype chimeric mice which allow tracking of IgM responses of allotype-marked B-1 and B-2 cells (61). In this experimental setup, endogenous B cells of the C57BL/6 background (IgH-b allotype) are depleted with allotype specific anti-IgM-b antibodies and replaced with transferred PerC B-1 of the IgH-a allotype which are refractory to the depletion antibodies and will engraft for the life of the animal. Following removal of the depleting antibodies, the endogenous B-2 cell population reemerge and are marked with anti-IgM-b antibodies, while the transferred B-1 cell are marked with anti-IgM-a antibodies (Fig 4C). Assessing antibody responses generated in IgH-allotype chimeric mice during a *T. gondii* infection revealed the presence of B-1 derived IgM-a antibodies that had low reactivity to *T. gondii* at days 14 and 30 post-infection, but the majority of highly reactive parasite-specific IgM-b was derived from the B-2 compartment (Fig 4D).

Attempts to explore the role of B-1 and B-2 cells utilizing B cell deficient muMT mice were complicated by their high susceptible to primary infection with the CEP strain, irrespective of whether they received PerC as neonates or splenic B-2 cells prior to the primary infection (Fig S5), thus underscoring the importance of B cells in resistance to *T. gondii* infection (18). Instead, mixed bone marrow chimeras were generated in which irradiated bumble or wildtype recipients were transferred wildtype or bumble bone marrow to reconstitute B-2 cells and the rest of the hematopoietic compartment. Since B-1a cells do not efficiently reconstitute irradiated recipients from adult bone marrow (62), some recipients received wildtype PerC to restore the B-1 compartment in this setting (59). These and other bone marrow chimeras (not shown) all succumbed to primary CEP infections (Fig S6). To bypass the susceptibility of irradiated bone marrow recipients to

live *T. gondii* infections (63), bone marrow chimeras were vaccinated with a replication deficient uracil auxotroph strain, which do not kill IFNγ-/- mice and provide protection to type I RH challenge (64, 65). Only recipient mice that received wildtype bone marrow were able to survive type I RH challenge (Fig 4E). Unexpectedly, when irradiated mice lacked *Nfkbid* in the hematopoietic compartment, they were highly susceptible to the vaccine strain (Fig S5). Hence, our reconstitution studies emphasize the importance of *Nfkbid* in humoral immunity to *T. gondii:* transfers of *Nfkbid* -sufficient PerC (B-1 cells, Fig 4A) or bone marrow (B-2 cells, Fig 4E) improve bumble's resistance to type I secondary infection, suggesting both compartments play a role in the immune response to the parasite. Interestingly, the study also suggests that *Nfkbid* is important in the non-hematopoietic lineage, as complete immunity was restored only when WT mice received WT BM cells (Fig S5).

Evidence for enhanced B-1 and B-2 cell activation in resistant A/J mice

Since *Nfkbid* has a profound effect on the maturation and activation of multiple B cell populations in the C57BL/6J background, we extended our analysis of B-1 and B-2 populations within the spleen and peritoneal cavity of A/J mice. Within the peritoneal B-1 cell compartment (CD19+, B220^{int}, CD11b+) increased percentages of CD5- B-1b cells were observed during secondary infection in resistant A/J mice, which appear to have downregulated their BCR as evidenced by being IgM^{lo} (Fig 5A, 5B). To further validate these findings, frequencies of CD5+ (B-1a) and CD5- (B-1b) cells within the CD43+ B-1 cell compartments of the peritoneum and spleen were determined, and a similar trend was observed (Fig 5C, 5D). In the spleen, both strains of mice had significantly increased frequencies of IgM-IgD- B-1a and B-1b cells in chronically infected animals compared to naïve, while in the peritoneum this increase was observed following challenge (Fig 5F). In these situations, resistant A/J mice often had two-fold greater percentages of IgM-IgD- B-

1 cells relative to the susceptible C57BL/6 mice. Following infection, B-1 cells in the spleens of A/J mice maintained high levels of BAFFR and TACI expression and expressed higher levels of surface CD138 relative to C57BL/6J mice (Fig 5E), markers known to be induced by *Nfkbid* and important for B cell activation and differentiation into antibody secreting cells (66). The B-2 compartment of A/J also showed enhanced activation. During secondary infection, although susceptible C57BL/6J and resistant A/J mice have similar frequencies of memory B cell CD73+ FCRL5- and atypical memory CD73+ FCRL5+ CD80+ populations (not shown), in A/J mice these compartments were significantly increased in their class-switch recombination frequencies (Fig 6A). The overall enhanced B cell activation profiles and class-switching in A/J mice was reflected in the parasite-specific serum antibody response to parasite lysate antigen. IgM and IgG antibodies were assessed by western blot from the resistant A/J background and showed significantly greater lysate antigen reactivity during secondary infections compared to C57BL/6J (Fig 6B-C). The roughly two-fold greater IgG reactivity to parasite antigen (Fig 6C) is consistent with enhanced class-switching in A/J mice observed by FACS (Fig 6A).

To generate a comprehensive view of immune response differences between A/J and C57BL/6 mice, many immune cell populations were characterized during chronic and secondary infections. Consistent with the increased parasite burdens observed in susceptible mice (Fig 1B, S1), greater frequencies of neutrophils, inflammatory macrophages, and dendritic cells were found in the peritoneal cavities and to a lesser extent within the spleens (not shown) of C57BL/6J compared to A/J mice on day 5 of secondary infection (Fig S7). Phenotypes associated with *Nfkbid* were further explored: T cell cytokine production (IL-2 and IFNγ). Although CD4 and CD8 T cell frequencies were not significantly different between the resistant and susceptible mouse backgrounds (Fig S7, not shown), an increase in peritoneal CD8 T cell in vitro recall production of IFNγ was

noted between A/J and C57BL/6J mice, however other parameters, including granzyme B and IL-2 expression were similar (Fig S8). Collectively these data suggest that while CD8 T cell production of IFNγ is enhanced in resistant mice and likely contributes to their resistance, B-2 and B-1 cells participate in a strikingly enhanced humoral response in A/J mice, offering insight into how immunity against parasitic infections may be achieved.

B-1 cells in resistant A/J mice have enhanced germline transcription of *Ighg* constant regions and different activation profiles

The diminished antibody response in bumble mice as well as the B cell phenotypic differences noted in A/J mice prompted us to investigate further how *Nfkbid* may be modulating the B cell compartment in the both genetic backgrounds. A transcriptomic approach was taken to define peritoneal B-1a, B-1b and B-2 cell response characteristics in resistant and susceptible mice during naïve, chronic and secondary infection states. The top differentially expressed genes commonly induced in B-1 and B-2 cells following infection are represented as a heatmap (Fig 7A), and the entire data set can be found in Table S4. GO term enrichment analysis found type I and II interferon signaling and immune defense signatures, including “response to protozoans”, as being enriched in the most differentially regulated genes among B cells following infection (Fig 7B), an observation consistent with the robust T cell IFNγ responses induced by *T. gondii* (Fig S8). Looking specifically at CD5- B-1 cells in A/J mice, which bore evidence for enhanced activation (Fig 5F), pathway enrichment analysis of genes differentially upregulated on day 5 of secondary infection compared to the naïve state found signatures of TLR-signaling, complement activation and somatic recombination (Fig S9). Germline transcription of *Ighg1*, *Ighg3*, *Ighg2b*, and *Ighg2a/c* was greatly enhanced in CD5- B-1 cells from A/J compared to C57BL/6J mice on day 5 of secondary infection (Fig 7C),

suggesting heightened isotype class switching occurred in mice on the resistant background, consistent with their IgM-IgD- phenotype (Fig 5E). Moreover *Cxcr3,* an important chemokine receptor for promoting Th1 and CD8 T cell responses during *T. gondii* infection (67-69), *Scimp* an adaptor for TLR4 signaling (70), *Semaphorin7* a noted inducer of inflammatory cytokines (71), the alarmins *S100a8* and *S100a9*, and genes associated with tissue tolerance including *Retnlg* and *Slpi,* were each specifically upregulated in CD5- B-1 cells from A/J compared to C57BL/6 mice on day 5 of challenge (Fig S9). Gene Set Enrichment Analysis (GSEA) of CD5- B-1 transcriptional variation between mice on day 5 of challenge detected correlation with gene sets that distinguish B cells following vaccination with different TLR-stimulating adjuvants (MPL vs R848), follicular vs early germinal center B cells, and tumor-associated immuno-suppressive dendritic cells (Fig 7D). In summary, the transcriptomics data suggest that the entire B cell compartment of both strains of mice experienced IFN-signaling during *T. gondii* infection. In the resistant A/J background but not in C57BL/6J mice, B-1 cells underwent Ig class switch recombination, perhaps through enhanced TLR-signaling.

Gene dosage of *Nfkbid* impacts parasite-specific IgG1 responses

Because A/J *Nfkbid* polymorphisms are largely found in non-coding regions (Table S3), we hypothesized that B cell differences observed in our system could be due to differences in *Nfkbid* expression levels. To investigate this possibility, we quantified *Nfkbid* expression within our transcriptomic dataset as well as by qPCR. B cells from C57BL/6J mice had greater expression of *Nfkbid* relative to A/J, particularly at the chronic infection stage (Fig 8A). Because *Nfkbid* expression differences could reflect heightened responsiveness to parasite load, we stimulated enriched peritoneal and splenic B cells

from A/J and C57BL/6J mice with LPS and noted that B cells from C57BL/6J mice had on average 1.5- to 2-fold greater induction of *Nfkbid* transcripts relative to A/J (Fig 8B).

To explore how gene dosage of *Nfkbid* impacts antibody responses generated against *T. gondii,* serum from chronically infected bumble heterozygotes (*Nfkbid*+/-), C57BL/6J, and A/J mice were analyzed. Although parasite-specific IgM and IgG3 did not differ between mouse strains, increased parasite-specific IgG1 and IgG2a/c serum responses were observed in A/J relative to C57BL/6 mice, a response that was phenocopied in particular for IgG1 in bumble heterozygotes (Fig 8C-D). In contrast, heterozygous expression of *Nfkbid* is sufficient to restore wildtype levels of parasite-specific IgM, IgG3, and IgG2b in mice with a C57BL/6 background when compared to bumble mice (Fig 4C, 7D). Hence, while *Nfkbid* is required for the generation of IgM and robust IgG responses against *T. gondii*, gene dosage of *Nfkbid* further controls IgG1 isotype profiles, presenting *Nfkbid* as tunable modulator of antibody IgG responses to parasites. Of note, when *Nfkbid+/-* mice were given secondary infections with the GT1 strain, all mice succumbed to the challenge (not shown), observations that are likely consistent with a multiple-QTL model for *T. gondii* immunity and apparent need for additional modifiers on chromosomes 10 and 17 to survive highly virulent challenges.

Discussion

The findings of this study underscore the utility of using inbred mouse panels to uncover novel determinants of immunity to parasites. An unbiased genetic screen identified *Nfkbid*, a tunable regulator of humoral responses to parasites. Within the C57BL/6J background, *Nfkbid* is required for maturation and class switching of B-2 cells during chronic *T. gondii* infection. While B-2 responses dominate the antibody response in this background, the lack of B-1 cells appear partially responsible for the immunity defect observed in bumble

mice. In contrast, survival against *T. gondii* infection in resistant mice correlates with a strong layered humoral response: enhanced activation and class-switching in both B-1 and B-2 cells. In this context, B-1 cells may assist the B-2 response to provide full immunity to challenge. The ability of B-1 cells to make parasite-specific antibodies, though of lower affinity, potentially amplifies B-2 immune responses to *T. gondii* through internalization of B-1 cell-derived antigen-antibody complexes (72), assisting MHCII antigen presentation for CD4 T cell help (73). Moreover, the effect of B cell-mediated immunity to *T. gondii* and other pathogens is likely underestimated in murine models using the C57BL/6 background, as enhanced B-1 and B-2 responses were primarily observed in A/J mice.

Though the exact pathway remains to be investigated, *Nfkbid* is downstream of TLR signaling in B cells (48, 49, 66), which in B-1a cells causes them to downregulate CD5 and facilitate differentiation into antibody secreting cells (60, 74). CD5 is a potent negative regulator of antigen receptor signaling that renders B-1a cells unresponsive to B cell receptor (BCR)-triggering (75). This inhibition is overcome by TLR-stimulation which causes CD5 to dissociate with the BCR, thereby releasing repression of BCR-mediated signaling and antibody secretion (74) against foreign- and self-antigen (60). These data suggest CD5- B-1b cells may represent an activated state of B-1 cells, and calls into question a strict division of labor between these two subsets (76). This supposition would fit several of the observations made in our system, including evidence for enhanced class switch recombination and TLR-gene signatures observed in the CD5- B-1 cells of the resistant background. In addition, BAFFR and TACI are known inducers of class-switch recombination (77), and increased expression of these receptors may further lower the threshold of activation and differentiation into CD138+ plasmablasts/plasma cells, all of which are regulated by *Nfkbid* (66) and occurring with greater magnitude in B-1 cells of

genetically resistant A/J mice. Although class switch recombination occurs with much greater frequency in B-2 cells of A/J mice, we found no evidence for enhanced expression of BAFFR and TACI in this compartment following *T. gondii* infection (not shown). Further investigation of pathways upstream of *Nfkbid,* such as the TLR pathway, has the potential to elucidate key requirements for *T. gondii* immunity.

Nfkbid appears to regulate transitional development in B-2 cells, which is analogous to previous findings in B-1 cells (48), but only evident following *T. gondii* infection. As immature B cells migrate out of the bone marrow to the spleen, there are several checkpoints which are controlled by NF-κB such as BCR- or BAFF-mediated signaling, both of which are known to induce *Nfkbid* expression (77, 78). Our observation of an accumulation of transitional B cells during *T. gondii* infection in bumble mice suggest *Nfkbid* plays a role in stabilizing advancement out of these developmental checkpoints. *Nfkbid* could act as a negative regulator of BCR signaling within B-2 cells, enabling pathogen-reactive B cells to develop beyond negative selection that would otherwise occur as antigen accumulate in secondary lymphoid organs over time. Alternatively, *Nfkbid* could be a positive regulator of NF-kB signaling, increasing the strength of BCR signaling to enable transitional B cells to become mature B cells. In both cases, a developmental defect likely restricts the pool of *T. gondii*-reactive mature B cells, preventing replenishment of antibody secreting cells during infection, culminating in the low parasite-specific antibody titers observed in bumble mice.

Heterologous immunity to a parasitic pathogen should, at a minimum, prevent disease against a wide variety of strains that differ in virulence or polymorphic antigens. An ideal parasite vaccine would entirely protect against re-infection and induce sterile immunity, thought possible since re-infection studies were first performed in mice (79) and humans immunized with irradiated sporozoites and *Plasmodium sp.* challenge (80-83).

Yet, only one partially protective vaccine is in use for any human parasitic pathogen, RTS,S/AS01, which has low efficacy for malaria prevention (84). Our results demonstrate that even in genetically resistant hosts, sterile immunity was not always achieved. Other loci that provide heterologous immunity to *T. gondii* include the MHC of A/J to certain strains like MAS and GUY-MAT. Whether *Tspan8* is the causal gene within the chr10 QTL (Mb 115.8-116.2) is unknown. *Tspan8* is one of four tetraspanins that encode four cysteines, including CD9 and CD81 known to influence B cell activation (85), but besides one report on impacting leukocyte migration (in the B6 background) (55), its role in immune function is unknown. *Tspan8* expression is highly expressed in epithelial cells, and we found no evidence for its expression in B cells by transcriptomic analysis and qPCR (not shown). Tetraspanins interact with integrins and play diverse roles in lymphocyte function (85). It is tempting to speculate that Tspan8 interacts with an unidentified lymphocyte integrin to mediate migration to the site of infection. Finally, the increased CD8 T cell IFNγ responses observed in resistant A/J mice are possibly the outcome from an unexplored QTL, as bumble and C57BL6/J mice have similar levels of IFNγ after *in vitro* recall (Fig S3). The genetic loci responsible for strain-dependent CD8 T cell IFNγ regulation during *T. gondii* infection remains to be determined.

The focus of this study was to use an unbiased genetic screen to find requirements for heterologous immunity to the most virulent strains of *T. gondii*. Our findings highlight the role of both innate and conventional B cells in humoral immunity to *T. gondii*, introducing B-1 cells as a potential vaccine target along with B-2 cells to maximize humoral immunity to parasitic infections. Moreover, we present a modulator of antibody responses against parasitic infections, *Nfkbid*, a transcriptional regulator that can tune B cell responses to provide an overall effective class-switched antibody response against parasites.

MATERIAL AND METHODS

Parasite strains and cell lines

Human foreskin fibroblasts (HFFs) monolayers were grown in DMEM (4.5 g/L D-glucose) (Life Technologies) supplemented with 2 mM L-glutamine, 20% fetal bovine serum (FBS) (Omega Scientific), 1% penicillin-streptomycin, and 0.2% gentamycin (Life Technologies). Mouse Embryonic Fibroblasts (MEFs) were grown in DMEM (4.5 g/L D-glucose) (Life Technologies) supplemented with 10% fetal bovine serum (FBS) (Omega Scientific), 20mM HEPES, 1% penicillin-streptomycin, and 0.2% gentamycin (Life Technologies). *Toxoplasma gondii* strains were passaged in HFFs in 'Toxo medium' (4.5 g/L D-glucose, L-glutamine in DMEM supplemented with 1% FBS and 1% penicillin-streptomycin). The following clonal strains were used (clonal types are indicated in parentheses): RH Δ*ku80* Δ*hxgprt* (type I), RH (1-1) *GFP::cLUC* (type I), GT1 (type I), GT1 *GFP::cLuc* (type I), and CEP *hxgprt*- (type III). The following atypical strains were used: MAS, MAS *GFP::cLuc* (2C8) (haplogroup 'HG' HG4), GUY-MAT (HG5), FOU (HG6), GPHT (HG6), TgCATBr5 (HG7), GUY-DOS (HG10), and VAND (HG10). The uracil auxotroph vaccine strain, RH *Δup Δompdc* (65), was passaged in HFFs in medium containing 250μM uracil.

Generation of GFP-expressing GT1 strains

GT1 parasites were transfected with linearized plasmids for parasite expression of GFP and click beetle luciferase (*GFP::cLUC*), parasites were grown on HFF monolayers in T-25 flasks in Toxo medium for 2 weeks. Parasites were removed from the flasks by scraping; the parasites were pelleted and washed with PBS and suspended in sterile FACS buffer (2% FBS in PBS). Fluorescent parasites where then sorted via fluorescence-activated cell sorting (FACS) into a 96-well plate with confluent HFF monolayers. To

ensure single plaque formation in at least one of the wells, the sort was titrated using the following parasite numbers: 100, 50, 25, 12, 6, 3, 2, and 1 for each well per row of 8.

Mice and ethics statement

Female C57BL/6J (H-2b), A/J (H-2a), C57BL/10SnJ (H-2b), B10.A-*H2*^{a} *H2-T18*^{a}/SgSnJ (H-2a), B6AF1/J (A/J x C57BL/6J F1 progeny), B6.129S2-*Ighm*^{tm1Cgn}/J (muMT), B6.SJL-*Ptprc*^{a} *Pepc*^{b}/BoyJ (CD45.1 congenic), B6.Cg-*Gpi1*^{a} *Thy1*^{a} *Igh*^{a}/J (IgH-a triple congenic mice), C57BL/6J-Chr7$^{A/J}$/NaJ and C57BL/6J-Chr10$^{A/J}$/NaJ (chromosome 7 and 10 consomic mice), and 26 (AxB;BxA) recombinant inbred (RI) mice derived from A/J and C57BL/6 founders, were purchased from Jackson Laboratories. The bumble mouse line used for this research project (49), C57BL/6J-*Nfkbid*^{m1Btlr}/Mmmh, RRID:MMRRC_036725-MU, was obtained from the Mutant Mouse Resource and Research Center (MMRRC) at University of Missouri, an NIH-funded strain repository, and was donated to the MMRRC by Bruce Beutler, M.D., University of Texas Southwestern Medical Center. Bumble mice were crossed to C57BL/6J to generate F1 bumble heterozygotes (*Nfkbid*+/-).

Mice were maintained under specific pathogen free conditions at UC Merced. Every effort was made to ensure unnecessary stress on the animals was avoided. Mouse work was performed in accordance with the National Institutes of Health Guide to the Care and Use of Laboratory Animals. All protocols have been reviewed and approved by UC Merced's Committee on Institutional Animal Care and Use Committee. UC Merced has an Animal Welfare Assurance filed with OLAW (#A4561-01), is registered with USDA (93-R-0518), and the UC Merced Animal Care Program is AAALAC accredited (001318).

Parasite infections

Parasite injections were prepared by scraping T-25 flasks containing vacuolated HFFs and sequential syringe lysis first through a 25G needed followed by a 27G needle. The

parasites were spun at 400 rpm for 5 min to remove debris and the supernatant was transferred, followed by a spin at 1700 rpm washing with PBS. For primary infections, mice were infected intraperitoneally (i.p.) with 10^4 tachyzoites of type III CEP *hxgprt-.* For some experiments, mice were vaccinated i.p. with 10^6 tachyzoites of RH *Δup Δompdc.* For secondary infections, mice were infected I.P. with $5x10^5$ type I parasites (RH or GT1). Parasite viability of the inoculum was determined by plaque assay following i.p. infections. In brief, 100 or 300 tachyzoites were plated in HFF monolayers grown in a 24-well plate and 4-6 days later were counted by microscopy (4x objective).

Blood plasma isolation and assessment of seroconversion

All mice were assessed for sero-positivity to *T. gondii* 4-5 weeks post primary infection. 50μL of blood was isolated from mice in tubes containing 5μL of 0.5M EDTA on ice, pelleted and the supernatant containing blood plasma was heat inactivated to denature complement at 56°C for 20 minutes and then stored at -80°C. HFFs were grown on coverslips and infected with GFP-expressing RH (1-1) overnight, fixed 18 hrs later with 3% formaldehyde (Polysciences) in PBS, washed, permeabilized and blocked with PBS containing 3% bovine serum albumin Fraction V (Sigma), 0.2M Triton X-100, 0.01% sodium azide, incubated with a 1:100 dilution of collected blood plasma for 2 hrs at room temperature, washed with PBS, and detected with Alexa Fluor 594-labeled secondary antibodies specific for mouse IgG (cat # A11032, Life Technologies). Seropositive parasites were observed by immunofluorescence microscopy (Nikon Eclipse Ti-U).

Brain superinfection assays and cyst enumeration

Brains from chronically infected mice (CEP *hxgprt-*) that survived secondary challenge were dissected, rinsed in PBS, passed through a 21G needle several times, pelleted and suspended in 1mL of PBS. For rederivation, 100μL of the brain homogenate was used to inoculate HFF monolayers in Toxo medium. One to two weeks later, infected HFFs were

syringe-lysed and plated on new HFF monolayers to encourage parasite growth. Once HFFs were fully vacuolated, parasites were passaged in Toxo medium supplemented with mycophenolic acid (MPA) and xanthine that selects for parasites encoding a functional *HXGPRT* (i.e. the challenging strains) and against the chronically infecting type III *hxgprt*- which lacks a functional *HXGPRT* gene. Outgrowth in MPA-xanthine was considered evidence for superinfection.

For counting tissue cysts, 100µl of brain homogenate was fixed in 900µL of ice cold methanol, incubated for 5 minutes in microtubes (MCT-175-C, Axygen), washed and stained overnight in a 500µL PBS solution containing 1:150 dilution of FITC-conjugated *Dolichos biflorus* agglutinin (Vector Laboratories) with slow rotation at 4°C. The stained homogenate was further washed and suspended in 1mL of PBS, of which several 50µL aliquots were counted by fluorescence microscopy, and the number of cysts per brain were deduced.

Genetic linkage analysis

Quantitative trait loci (QTL) analysis was performed with the package r/QTL in R (version 3.6.1). LOD scores for each marker were calculated using the Haley-Knott regression model with the function 'scanone', or for all possible combination of two markers (i.e. epistatic interactions) using the function 'scantwo'. 1000 permutations were performed to obtain the genome wide LOD threshold for a P value of ≤0.05, which was considered statistically significant. Similar results were obtained with a linear mixed regression model. To estimate the effect each QTL had on the overall phenotype, the function 'fitqtl' was first used to fit the data to a multiple-QTL model. Statistical support was found for inclusion of all four QTLs with LOD scores > 3 compared to any lesser combination of three-QTLs (ANOVA P <0.02). Individual QTL effects were then calculated under the assumption of

the four-QTL model, which collectively accounts for 91% of the observed phenotypic variance.

Cell isolation, in *vitro* recall infections, and FACS analysis

PECs were isolated by peritoneal lavage and splenocytes obtained, as described in (38). In brief, 4mL of FACS buffer (PBS with 1% FBS) and 3mL of air were injected into the peritoneal cavity with a 27G needle. After agitation, the PEC wash was poured into a conical tube. PEC washes were filtered through a 70μm cell strainer, pelleted, and washed with FACS buffer before staining. Spleens were dissected and crushed through 70μm cell strainers, pelleted, incubated in ACK red blood cell RBC lysis buffer (0.15M NH_4Cl, 10mM $KHCO_3$, 0.1mM EDTA) for 5 minutes at room temperature, then washed with FACS buffer. To obtain peripheral blood leukocytes (PBLs), 50μL of blood was isolated from mice in tubes containing 5μL of 0.5 M EDTA on ice, pelleted and incubated in ACK lysis buffer, washed and peripheral blood leukocytes (PBLs) were suspended in FACS buffer.

For FACS analysis, all preparations were done on ice, and cells were blocked in FACS buffer containing Fc Block anti-CD16/32 (2.4G2) (BD Biosciences), 5% normal hamster serum, and 5% normal rat serum (Jackson ImmunoResearch) for 20 minutes prior to staining with fluorophore-conjugated monoclonal antibodies (mAbs). The following mAbs (1:100 staining dilutions) were used: anti-CD1d-BV650 (1B1, BD Bioscience), anti-CD11c-eFlour 450 (N418, eBioscience); anti-CD11c-eFlour 450 (N418, BD Bioscience); anti-CD45.2-eFlour 450 (104, eBioscience); anti-CD4-eFlour 450 (GK1.5, eBioscience), anti-CD4-PECy7 (GK1.5, eBioscience); anti-CD11b-FITC (M1/70, eBioScience), anti-CD11b-BUV395 (M1/70, BD Bioscience), anti-CD11b-BV421 (M1/70, BD Bioscience), anti-CD11b-Pacific Blue (M1/70, BioLegend); anti-IFNγ-PE (XMG1.2, BD Bioscience); anti-CD8α-APC (53-6.7, eBioscience), anti-CD8α-BV510 (53-6.7, BioLegend), anti-Ly6G-APC (1A8-Ly6g, eBioscience), anti-CD19-PerCP-Cy5.5 (ebio1D3, eBioscience), anti-

CD19-PE (6D5, BioLegend), anti-CD19-BV785 (6D5, BioLegend), anti-CD3-eFlour 780 (17A2, BD Biosciences), anti-Ly6C-PECy7 (HK1.4, BioLegend), anti-CD23-Pacific Blue (B3B4, BioLegend), anti-CD23-AF700 (B3B4, BioLegend), anti-CD21/CD35-FITC (7E9, BioLegend), anti-CD21/CD35-PE (7E9, BioLegend), anti-CD5-APC (53-7.3, BioLegend), anti-CD43-BV510 (S7, BD Bioscience), anti-CD43-BUV737 (S7, BD Bioscience), anti-CD5-PerCP-Cy5.5 (53-7.3, BioLegend), anti-CD5- Cy7-APC (53-7.3, BioLegend), anti-CD45R/B220-Cy7-APC (RA3-6B2, anti-CD45R/B220-BUV-661 (RA3-6B2, BD Bioscience), anti-CD73-Cy7-PE (eBioTY/11.9, eBioscience), anti-CD80-BV711 (16-10A1, BioLegend), anti-FCRL5-af88 (polyclonal, R&D systems) anti-IgM-PECy7 (RMM-1, BioLegend), anti-IgM-BV605 (RMM-1, BioLegend), anti-IgD-FITC (11-26c.2a, BioLegend), anti-IgD-PEDazzle (11-26c.2a, BioLegend), anti-CD138/Syndecan-1-BV510 (281-2, BD Bioscience), anti-CD138/Syndecan-1-BV650 (281-2, BioLegend), anti-mouse-CD267/TACI-AlexaFlour-647 (8F10, BD Biosciences), and anti-CD268/BAFF-R-PE (7H22-E16, BioLegend). Other FACS reagents included the viability dye propidium iodide (Sigma) at a final concentration of 1µg/mL.

For *in vitro* recall, splenocytes and PerC were isolated from chronic and challenged mice (day 5 or 7 following secondary infection) and 6 x 10^5 cells per well (96-well plate) were plated in T cell medium (RPMI 1640 with GlutaMAX, 20% FBS, 1% Pen/Strep, 1mM NaPyruvate, 10mM HEPES, 1.75µl BME). Cells were infected with a type I strain (RH or GT1) strain at an MOI (multiplicity of infection) of 0.2 for 18 hr; 3µg/mL brefeldin A (eBioscience) was added for the last 5 hr of infection. 96-well plates were placed on ice, cells were harvested by pipetting and washed with FACS buffer, blocked, and stained for surface markers. Cells were fixed with BD Cytofix/Cytoperm and permeabilized with BD Perm/Wash solution (cat# 554714, BD Pharmingen), stained with anti-IFNγ-PE (XMG1.2, BD Bioscience), anti-GZB (GB11, BioLegend) and anti-IL-2-APC (JES6-5H4, BioLegend)

on ice for 1 hr or overnight. Cells were then washed once with BD Perm/Wash solution, once in FACS buffer, and analyzed by FACS.

For FoxP3 staining, peritoneal lavage was performed on chronic and challenged (day 7 following secondary infection) bumble and WT mice. Cells were washed and surface stained. Fixation and permeabilization was performed with the eBioscience Foxp3/Transcription Factor Staining Buffer Set (cat # 00-5523-00) before intracellular staining with anti-Foxp3-PE (MF-14, BioLegend) according to the manufacturer's recommendations. Flow cytometry was performed on a Beckman Coulter Cytoflex LX, LSR II (BD Biosciences), or the Bio-Rad ZE5 and analyzed with FlowJo™ software.

Analysis of isotype-specific antibody reactivity to *Toxoplasma gondii* by flow cytometry

For serum reactivity analysis, syringe-lysed GFP-expressing strains (RH1-1 and GT1-GFP) were fixed in 3% formaldehyde for 20 minutes, washed twice in PBS, and plated in 96 well micro-titer plates at $4x10^5$ parasites/well. The parasites were then incubated with serum from chronically infected mice, at serum concentrations ranging from 10^{-2} to 10^{-6} diluted in FACS buffer, for 20 minutes at 37°C. Parasites were then washed with FACS buffer and placed on ice for incubation with anti-isotype detection antibodies depending on application: anti-IgG3-BV421 (R40-82, BD Bioscience), anti-IgM-PE/Cy7 (RMM-1, BioLegend), anti-IgG1-FITC (RMG1-1, BioLegend), anti-IgG1-APC (RMG1-1, BioLegend), anti-IgG2b-FITC (RMG2b-1, BioLegend), anti-IgG2b-PE (RMG2b-1, BioLegend), anti-IgG2a-FITC (RMG2a-62, BioLegend), anti-IgG2a-PerCP/Cy5.5 (RMG2a-62, BioLegend), anti-IgM-a-PE (DS-1, BD Bioscience), Anti-IgM-b-PE (AF6-78, BD Bioscience).

Parasite neutralization assay

Heat-inactivated serum was used to coat live parasites for 20 minutes at 37°C before infecting $5x10^5$ mouse embryonic fibroblasts/well (MEFs) in 96 well plates. Immediately following addition of parasite to MEF wells, plates were spun at 1200rpm for 3 minutes to synchronize infection. 2 hrs after initiation of infection, cells were placed on ice and harvested by scraping with pipette tips. Cells were washed twice in FACS buffer, suspended in 1:1000 PI in FACS buffer, and then analyzed by flow cytometry.

SDS-PAGE and immunoblotting for parasite lysate antigen

To generate parasite lysate antigens *Toxoplasma gondii* was cultured in HFF and expanded to approximately $2x10^8$ parasites. Parasites were syringe-lysed, washed with sterile 1X PBS and the parasite pellet was lysed with (1mL) 0.1% TritonX-100 detergent in 1X PBS. Solubilized parasites were centrifuged at 2,000 RCF for 20 minutes to remove large debris. The supernatant was aliquoted and stored at -80°C. Parasite lysate was reduced with β-mercaptoethanol (BME) and separated via SDS-PAGE in 4-20% Mini-PROTEAN TGX pre-cast gels (cat # 4561096, Bio-Rad) before transfer to PVDF membrane using a Trans-Blot Turbo Mini PVDF Transfer Pack (cat # 1704156, Bio-Rad) via Bio-Rad Transblot Turbo (cat # 1704150, Bio-Rad). Membranes were blocked with 10% fortified bovine milk dissolved in Tris-Buffered Saline with 0.1% Tween (TBS-T 0.1%) for 1-2 hrs at room temperature or overnight at 4°C. Blots were then probed with heat-inactivated serum in block at either 1:1,000 dilution for serum IgM analysis or 1:5,000 dilution for serum IgG analysis overnight at 4°C. Membranes were washed with TBS-T 0.1% three times for 20 minutes per wash. Blots were then incubated for one hr at room temperature with goat α-mouse horseradish peroxidase (HRP)-conjugated antibodies (SouthernBiotec): anti-IgM secondary 1:1000 (cat# 1020-05) and total anti-IgG secondary 1:5000 (cat# 1030-05). Membranes were then washed with TBS-T 0.1% three times and developed with Immobilon® Forte Western HRP Substrate (WBLUF0500). All blots were

imaged via chemiluminescence on a ChemiDoc Touch (cat# 12003153, Bio-Rad). Image Lab 6.1 software (Bio-Rad) was used for analysis of bands and total lane signal. Western blots comparing A/J to C57BL/6J were developed simultaneously and the band signal was normalized to A/J.

RNA isolation and sequencing

Peritoneal B-1a (B220$^{int-neg}$ CD19^{high} CD11b+ CD5+ PI-), B-1b (B220$^{int-neg}$ CD19^{high} CD11b+ CD5- PI-), or B-2 B cells (B220^{high} CD19+ CD11b- PI-) were sorted into 500ul RNeasy lysis buffer using a FACS ARIA II cell sorter (BD Biosciences). RNA was purified using the RNeasy mini kit (cat# 74134, Qiagen) according to the manufacturer's protocol. RNA purity was tested by Qubit (ThermoFisher) and Agilent 2100 BioAnalyzer for total RNA with picogram sensitivity. DNA libraries were generated with a Lexogen QuantSeq-UMI FWD 3′ mRNA-Seq Library Prep Kit (cat# 015). Samples were sent to UC Davis for QuantSeq 3' mRNA FWD-UMI sequencing.

Gene expression analysis and data availability

Raw reads were trimmed and mapped by the BlueBee genomic pipeline FWD-UMI Mouse (GRCm38) Lexogen Quantseq 2.6.1 (Lexogen). In brief, reads were quality controlled with 'FASTQC', trimmed with 'Bbduk' to remove low quality tails, poly(A)read-through and adapter contaminations, read alignments to the *Mus musculus* genome build GRCm38 were done with 'STAR', and gene reads were quantified with 'HTSeq-count'. Differentially expressed gene (DEG) analysis was performed utilizing limma-voom in R version 3.6.3 in RStudio with Bioconductor suite of packages. Heatmaps were generated with 'gplots'. Pathway and GO term analysis was performed with MouseMine (mousemine.org), and gene set enrichment analysis was performed with GSEA v4.0.3. RNA-sequencing data generated in this study has been deposited in the NCBI Sequence Read Archive

(Bioproject accession number PRJNA637442). All other data that support the findings herein are available from the corresponding author upon reasonable request.

LPS-stimulation of enriched B cells and quantitative PCR

PerC and splenocytes were isolated from naïve 6-8 week-old C57BL/6J and A/J mice and enriched for B cells using the EasySep Mouse Pan B cell Isolation Kit (cat#19844, StemTech). Bead enrichment for splenic samples had the addition of biotinylated anti-CD43 antibodies (clone S7, BD Bioscience) to remove B-1 cells. Enriched samples were plated in a 96-well plate at 400,000 cells per well and stimulated with 25ug/ml of LPS (cat# L4391-1MG, Sigma). After 2 hrs, total RNA was isolated using the Rneasy Mini Kit (cat# 74134) and cDNA was synthesized using High Capacity cDNA Reverse Transcription Kit (ThermoFisher, cat#4368814). Quantitative PCR was performed on synthesized cDNA samples using ThermoFisher TaqMan Master Mix (cat# 4444556) and TaqMan probes: *Actb* - Assay ID:Mm02619580_g1 (cat# 4331182), and *Nfkbid* - Assay ID: Mm00549082_m1 (cat# 4331182), according to the manufacturer's protocol. Normalization of *Nfkbid* expression in each sample was calculated in comparison to *Actb* expression levels. Fold change in *Nfkbid* expression of AJ relative to that of C57BL/6J cells was determined through the delta delta CT method ($2^{-\Delta\Delta CT}$).

PerC adoptive transfers and IgH allotype chimeric mouse generation

PerC was harvested by peritoneal lavage of 6-12 week old C57BL/6J donor mice as described above and $5x10^6$ total peritoneal exudate cells (total PerC)/60ul PBS dose were transferred i.p. into 2-4 day old bumble neonates. Allotype chimeric mouse generation was performed as previously described (61). In brief, 1-day old C57BL/6J neonates were treated with 0.1mg of anti-IgM-b (clone AF6-78) and twice weekly thereafter treated with 0.2mg of anti-IgM-b for 6 weeks. On day 2 after birth the neonates were given $5x10^6$ total

PerC from B6.Cg-*Gpi1*^{a} *Thy1*^{a} *Igh*^{a} delivered i.p. The mice were then allowed to rest for 6 weeks after the last antibody treatment before infection with *T. gondii*.

Bone marrow chimeric mice generation

B6.SJL-*Ptprc*^{a} *Pepc*^{b}/BoyJ, bumble, and C57BL/6J recipient mice were given 2 doses of 500cGy with an X-Rad320 (Precision X-Ray) with a 4 hr interval. Donor BM cells were harvested from muMT, bumble and WT C57BL/6J mice, filtered with a 70um filter, incubated in ACK red blood cell lysis buffer, washed with PBS and transplanted by retro-orbital injection at a concentration of 10^7 cells/200ul PBS dose. For mixed BM chimeras, 1:1 mixtures of muMT and bumble or muMT and WT BM cells were created. Recipient mice were then allowed to rest for 8 weeks. Reconstitution was assessed at 8 weeks by FACS analysis of PBL.

ELISA

High-affinity protein binding microplates (Corning) were coated overnight goat anti-mouse IgM (1mg/ml, Southern Biotech, cat# 1021-01) and blocked with coating buffer containing with 1% BSA (w/v) and 2% goat serum (Omega Scientific) in PBS. Wells were washed with ELISA wash buffer (1X PBS, 0.05% TweenTM-20). Mouse serum samples were diluted 1:400 in coating buffer and incubated in the wells for 1 hr. Wells were washed 5 times and secondary goat anti-IgM-HRP (Southern Biotech, cat# 1021-08) at 1:5000 dilution was incubated for 1 hr in the wells. Wells were washed several times and developed with TMB substrate (Invitrogen). Development was stopped after 20 minutes with 1M H_3PO_4 stop solution. Absorbance was measured at 450nm on a BioTek Epoch microplate spectrophotometer.

Statistics

Statistical analysis was performed with Graphpad Prism 8 software. Statistical significance was defined as $P < 0.05$. P values were calculated using paired or unpaired two-tailed t-

tests, 2-way ANOVA with Tukey multiple comparison correction, and multiple t-tests with the Holm-Sidak correction for multiple comparisons. Survival curve significance was calculated using log-rank (Mantel-Cox) testing. Significance in time to death was calculated using the Gehan-Breslow-Wilcoxon test. Differential gene expression analysis statistics were calculated using the Limma-Voom R package, P values were adjusted with the Benjamini-Hochberg correction for multiple comparisons. GO term and pathway enrichment analysis statistics were performed at mousemine.org using the Holm-Bonferroni test correction. Statistical methods used for each figure are indicated in the figure legends.

Acknowledgments

This work was supported by NIH grants R01 AI137126, R15 AI131027, a Hellmann Fellowship and an MCB departmental award to KJ; and by NIH grants U19-AI109962 and R01 AI117890 to NB. The sequencing was carried out at the DNA Technologies and Expression Analysis Cores at the UC Davis Genome Center, supported by NIH Shared Instrumentation Grant 1S10OD010786-01. We would like to thank David Gravano and the UC Merced Stem Cell Instrumentation Foundry for their assistance designing panels and utilizing instruments, supported by the DoD Research and Education Program for HBCU/MSI Instrumentation Grant W911NF1910529. The authors declare no conflict of interest.

REFERENCES

1. Sacks DL (2014) Vaccines against tropical parasitic diseases: A persisting answer to a persisting problem. *Nat Immunol* 15(5): 403-405.

2. Lorenzi H*, et al* (2016) Local admixture of amplified and diversified secreted pathogenesis determinants shapes mosaic toxoplasma gondii genomes. *Nat Commun* 7: 10147.

3. Howe DK & Sibley LD (1995) Toxoplasma gondii comprises three clonal lineages: Correlation of parasite genotype with human disease. *J Infect Dis* 172(6): 1561-1566.
4. Khan A, *et al* (2006) Genetic divergence of toxoplasma gondii strains associated with ocular toxoplasmosis, brazil. *Emerg Infect Dis* 12(6): 942-949.

5. McLeod R, *et al* (2012) Prematurity and severity are associated with toxoplasma gondii alleles (NCCCTS, 1981-2009). *Clin Infect Dis* 54(11): 1595-1605.

6. Grigg ME, Ganatra J, Boothroyd JC & Margolis TP (2001) Unusual abundance of atypical strains associated with human ocular toxoplasmosis. *J Infect Dis* 184(5): 633 639.

7. Campos MAS, *et al* (2008) Ocular sequelae of congenital toxoplasmosis in brazil compared with europe. *PLoS Neglected Tropical Diseases* 2(8): e277.

8. Suzuki Y & Remington JS (1988) Dual regulation of resistance against toxoplasma gondii infection by lyt-2+ and lyt-1+, L3T4+ T cells in mice. *J Immunol* 140(11): 3943-3946.

9. Suzuki Y & Remington JS (1990) The effect of anti-IFN-gamma antibody on the protective effect of lyt-2+ immune T cells against toxoplasmosis in mice. *J Immunol* 144(5): 1954-1956.

10. Gazzinelli RT, Hakim FT, Hieny S, Shearer GM & Sher A (1991) Synergistic role of CD4+ and CD8+ T lymphocytes in IFN-gamma production and protective immunity induced by an attenuated toxoplasma gondii vaccine. *J Immunol* 146(1): 286-292.

11. Gigley JP, Fox BA & Bzik DJ (2009) Cell-mediated immunity to toxoplasma gondii develops primarily by local Th1 host immune responses in the absence of parasite replication. *J Immunol* 182(2): 1069-1078.

12. Jordan KA, *et al* (2009) Kinetics and phenotype of vaccine-induced CD8+ T-cell responses to toxoplasma gondii. *Infect Immun* 77(9): 3894-3901.

13. Gigley JP, Bhadra R & Khan IA (2011) CD8 T cells and toxoplasma gondii: A new paradigm. *J Parasitol Res* 2011: 243796.

14. Khan IA, Hwang S & Moretto M (2019) Toxoplasma gondii: CD8 T cells cry for CD4 help. *Front Cell Infect Microbiol* 9: 136.

15. Casciotti L, Ely KH, Williams ME & Khan IA (2002) CD8(+)-T-cell immunity against toxoplasma gondii can be induced but not maintained in mice lacking conventional CD4(+) T cells. *Infect Immun* 70(2): 434-443.

16. Johnson LL & Sayles PC (2002) Deficient humoral responses underlie susceptibility to toxoplasma gondii in CD4-deficient mice. *Infect Immun* 70(1): 185-191.

17. Chen M, *et al* (2003) Induction of protective immunity by primed B-1 cells in toxoplasma gondii -infected B cell-deficient mice. *Microbiol Immunol* 47(12): 997-1003.

18. Kang H, Remington JS & Suzuki Y (2000) Decreased resistance of B cell-deficient mice to infection with toxoplasma gondii despite unimpaired expression of IFN-gamma, TNF-alpha, and inducible nitric oxide synthase. *J Immunol* 164(5): 2629-2634.

19. Sayles PC, Gibson GW & Johnson LL (2000) B cells are essential for vaccination-induced resistance to virulent toxoplasma gondii. *Infect Immun* 68(3): 1026-1033.

20. Couper KN, Roberts CW, Brombacher F, Alexander J & Johnson LL (2005) Toxoplasma gondii-specific immunoglobulin M limits parasite dissemination by preventing host cell invasion. *Infect Immun* 73(12): 8060-8068.

21. Mineo JR, *et al* (1993) Antibodies to toxoplasma gondii major surface protein (SAG-1, P30) inhibit infection of host cells and are produced in murine intestine after peroral infection. *J Immunol* 150(9): 3951-3964.

22. Joiner KA, Fuhrman SA, Miettinen HM, Kasper LH & Mellman I (1990) Toxoplasma gondii: Fusion competence of parasitophorous vacuoles in fc receptor-transfected fibroblasts. *Science* 249(4969): 641-646.

23. Mordue DG, Hakansson S, Niesman I & Sibley LD (1999) Toxoplasma gondii resides in a vacuole that avoids fusion with host cell endocytic and exocytic vesicular trafficking pathways. *Exp Parasitol* 92(2): 87-99.

24. Zhao Y, Marple AH, Ferguson DJ, Bzik DJ & Yap GS (2014) Avirulent strains of toxoplasma gondii infect macrophages by active invasion from the phagosome. *Proc Natl Acad Sci U S A* 111(17): 6437-6442.

25. Glatman Zaretsky A, *et al* (2012) Infection with toxoplasma gondii alters lymphotoxin expression associated with changes in splenic architecture. *Infect Immun* 80(10): 3602-3610.

26. Park J, *et al* (2019) Impact of interleukin-27p28 on T and B cell responses during toxoplasmosis. *Infect Immun* 87(12): 10.1128/IAI.00455-19. Print 2019 Dec.
27. Stumhofer JS, Silver JS & Hunter CA (2013) IL-21 is required for optimal antibody production and T cell responses during chronic toxoplasma gondii infection. *PLoS One* 8(5): e62889.

28. Smith FL & Baumgarth N (2019) B-1 cell responses to infections. *Curr Opin Immunol* 57: 23-31.

29. Alugupalli KR, *et al* (2004) B1b lymphocytes confer T cell-independent long-lasting immunity. *Immunity* 21(3): 379-390.

30. Haas KM, Poe JC, Steeber DA & Tedder TF (2005) B-1a and B-1b cells exhibit distinct developmental requirements and have unique functional roles in innate and adaptive immunity to S. pneumoniae. *Immunity* 23(1): 7-18.

31. Gil-Cruz C, *et al* (2009) The porin OmpD from nontyphoidal salmonella is a key target for a protective B1b cell antibody response. *Proc Natl Acad Sci U S A* 106(24): 9803-9808.

32. Cunningham AF, *et al* (2014) B1b cells recognize protective antigens after natural infection and vaccination. *Front Immunol* 5: 535.

33. Yang Y, *et al* (2012) Antigen-specific antibody responses in B-1a and their relationship to natural immunity. *Proc Natl Acad Sci U S A* 109(14): 5382-5387.

34. Pape KA, Taylor JJ, Maul RW, Gearhart PJ & Jenkins MK (2011) Different B cell populations mediate early and late memory during an endogenous immune response. *Science* 331(6021): 1203-1207.

35. Krishnamurty AT, *et al* (2016) Somatically hypermutated plasmodium-specific IgM(+) memory B cells are rapid, plastic, early responders upon malaria rechallenge. *Immunity* 45(2): 402-414.

36. Elbez-Rubinstein A, *et al* (2009) Congenital toxoplasmosis and reinfection during pregnancy: Case report, strain characterization, experimental model of reinfection, and review. *J Infect Dis* 199(2): 280-285.

37. Jensen KD, *et al* (2015) Toxoplasma gondii superinfection and virulence during secondary infection correlate with the exact ROP5/ROP18 allelic combination. *MBio* 6(2): 2280.

38. Splitt SD, *et al* (2018) PD-L1, TIM-3, and CTLA-4 blockade fail to promote resistance to secondary infection with virulent strains of toxoplasma gondii. *Infect Immun*

39. Fux B, *et al* (2007) Toxoplasma gondii strains defective in oral transmission are also defective in developmental stage differentiation. *Infect Immun* 75(5): 2580-2590.

40. Su C, *et al* (2003) Recent expansion of toxoplasma through enhanced oral transmission. *Science* 299(5605): 414-416.

41. McLeod R, Skamene E, Brown CR, Eisenhauer PB & Mack DG (1989) Genetic regulation of early survival and cyst number after peroral toxoplasma gondii infection of A x B/B x A recombinant inbred and B10 congenic mice. *J Immunol* 143(9): 3031-3034.

42. Jensen KD, *et al* (2013) Toxoplasma gondii rhoptry 16 kinase promotes host resistance to oral infection and intestinal inflammation only in the context of the dense granule protein GRA15. *Infect Immun* 81(6): 2156-2167.

43. Brown CR, *et al* (1995) Definitive identification of a gene that confers resistance against toxoplasma cyst burden and encephalitis. *Immunology* 85(3): 419-428.

44. Brown CR & McLeod R (1990) Class I MHC genes and CD8+ T cells determine cyst number in toxoplasma gondii infection. *J Immunol* 145(10): 3438-3441.

45. Hassan MA, Butty V, Jensen KD & Saeij JP (2014) The genetic basis for individual differences in mRNA splicing and APOBEC1 editing activity in murine macrophages. *Genome Res* 24(3): 377-389.

46. Hassan MA, *et al* (2015) Transcriptional and linkage analyses identify loci that mediate the differential macrophage response to inflammatory stimuli and infection. *PLoS Genet* 11(10): e1005619.

47. Schuster M, Annemann M, Plaza-Sirvent C & Schmitz I (2013) Atypical IkappaB proteins - nuclear modulators of NF-kappaB signaling. *Cell Commun Signal* 11(1): 23-23.

48. Touma M, *et al* (2011) Impaired B cell development and function in the absence of IkappaBNS. *J Immunol* 187(8): 3942-3952.

49. Arnold CN, *et al* (2012) A forward genetic screen reveals roles for nfkbid, Zeb1, and Ruvbl2 in humoral immunity. *Proc Natl Acad Sci U S A* 109(31): 12286-12293.

50. Pedersen GK, *et al* (2016) Heterozygous mutation in IkappaBNS leads to reduced levels of natural IgM antibodies and impaired responses to T-independent type 2 antigens. *Front Immunol* 7: 65.

51. Touma M, *et al* (2007) Functional role for I kappa BNS in T cell cytokine regulation as revealed by targeted gene disruption. *J Immunol* 179(3): 1681-1692.

52. Schuster M, *et al* (2012) IkappaB(NS) protein mediates regulatory T cell development via induction of the Foxp3 transcription factor. *Immunity* 37(6): 998-1008.

53. Kuwata H, *et al* (2006) IkappaBNS inhibits induction of a subset of toll-like receptor-dependent genes and limits inflammation. *Immunity* 24(1): 41-51.

54. Berthier-Vergnes O, *et al* (2011) Gene expression profiles of human melanoma cells with different invasive potential reveal TSPAN8 as a novel mediator of invasion. *Br J Cancer* 104(1): 155-165.

55. Zhao K, Wang Z, Hackert T, Pitzer C & Zoller M (2018) Tspan8 and Tspan8/CD151 knockout mice unravel the contribution of tumor and host exosomes to tumor progression. *J Exp Clin Cancer Res* 37(1): 312-6.

56. Kim CC, Baccarella AM, Bayat A, Pepper M & Fontana MF (2019) FCRL5(+) memory B cells exhibit robust recall responses. *Cell Rep* 27(5): 1446-1460.e4.

57. Pedersen GK, *et al* (2014) B-1a transitional cells are phenotypically distinct and are lacking in mice deficient in IkappaBNS. *Proc Natl Acad Sci U S A* 111(39): 4119.

58. Baumgarth N, Jager GC, Herman OC & Herzenberg LA (2000) CD4+ T cells derived from B cell-deficient mice inhibit the establishment of peripheral B cell pools. *Proc Natl Acad Sci U S A* 97(9): 4766-4771.

59. Choi YS & Baumgarth N (2008) Dual role for B-1a cells in immunity to influenza virus infection. *J Exp Med* 205(13): 3053-3064.

60. Kreuk LS, *et al* (2019) B cell receptor and toll-like receptor signaling coordinate to control distinct B-1 responses to both self and the microbiota. *Elife* 8: 10.7554/eLife.47015.

61. Lalor PA, Herzenberg LA, Adams S & Stall AM (1989) Feedback regulation of murine ly-1 B cell development. *Eur J Immunol* 19(3): 507-513.

62. Kantor AB, Stall AM, Adams S, Herzenberg LA & Herzenberg LA (1992) Differential development of progenitor activity for three B-cell lineages. *Proc Natl Acad Sci U S A* 89(8): 3320-3324.

63. Yap GS & Sher A (1999) Effector cells of both nonhemopoietic and hemopoietic origin are required for interferon (IFN)-gamma- and tumor necrosis factor (TNF)-alpha-dependent host resistance to the intracellular pathogen, toxoplasma gondii. *J Exp Med* 189(7): 1083-1092.

64. Fox BA & Bzik DJ (2002) De novo pyrimidine biosynthesis is required for virulence of toxoplasma gondii. *Nature* 415(6874): 926-929.

65. Fox BA & Bzik DJ (2010) Avirulent uracil auxotrophs based on disruption of orotidine-5'-monophosphate decarboxylase elicit protective immunity to toxoplasma gondii. *Infect Immun* 78(9): 3744-3752.

66. Khoenkhoen S, *et al* (2019) TACI expression and plasma cell differentiation are impaired in the absence of functional IkappaBNS. *Immunol Cell Biol* 97(5): 485-497.

67. Chu HH, *et al* (2016) Continuous effector CD8(+) T cell production in a controlled persistent infection is sustained by a proliferative intermediate population. *Immunity* 45(1): 159-171.

68. Cohen SB, *et al* (2013) CXCR3-dependent CD4(+) T cells are required to activate inflammatory monocytes for defense against intestinal infection. *PLoS Pathog* 9(10): e1003706.

69. Shah S, Grotenbreg GM, Rivera A & Yap GS (2015) An extrafollicular pathway for the generation of effector CD8(+) T cells driven by the proinflammatory cytokine, IL-12. *Elife* 4: 10.7554/eLife.09017.

70. Luo L, *et al* (2017) SCIMP is a transmembrane non-TIR TLR adaptor that promotes proinflammatory cytokine production from macrophages. *Nat Commun* 8: 14133.

71. Suzuki K, *et al* (2007) Semaphorin 7A initiates T-cell-mediated inflammatory responses through alpha1beta1 integrin. *Nature* 446(7136): 680-684.

72. Nguyen TT, *et al* (2017) The IgM receptor FcmuR limits tonic BCR signaling by regulating expression of the IgM BCR. *Nat Immunol* 18(3): 321-333.

73. Blandino R & Baumgarth N (2019) Secreted IgM: New tricks for an old molecule. *J Leukoc Biol* 106(5): 1021-1034.

74. Savage HP, *et al* (2019) TLR induces reorganization of the IgM-BCR complex regulating murine B-1 cell responses to infections. *Elife* 8: 10.7554/eLife.46997.

75. Bikah G, Carey J, Ciallella JR, Tarakhovsky A & Bondada S (1996) CD5-mediated negative regulation of antigen receptor-induced growth signals in B-1 B cells. *Science* 274(5294): 1906-1909.

76. Baumgarth N (2016) B-1 cell heterogeneity and the regulation of natural and antigen-induced IgM production. *Front Immunol* 7: 324.

77. Castigli E, *et al* (2005) TACI and BAFF-R mediate isotype switching in B cells. *J Exp Med* 201(1): 35-39.

78. Rowland SL, Leahy KF, Halverson R, Torres RM & Pelanda R (2010) BAFF receptor signaling aids the differentiation of immature B cells into transitional B cells following tonic BCR signaling. *J Immunol* 185(8): 4570-4581.

79. Nussenzweig RS, Vanderberg J, Most H & Orton C (1967) Protective immunity produced by the injection of x-irradiated sporozoites of plasmodium berghei. *Nature* 216(5111): 160-162.

80. Rieckmann KH (1990) Human immunization with attenuated sporozoites. *Bull World Health Organ* 68 Suppl: 13-16.

81. Hoffman SL, *et al* (2002) Protection of humans against malaria by immunization with radiation-attenuated plasmodium falciparum sporozoites. *J Infect Dis* 185(8): 1155-1164.

82. Rieckmann KH, Carson PE, Beaudoin RL, Cassells JS & Sell KW (1974) Letter: Sporozoite induced immunity in man against an ethiopian strain of plasmodium falciparum. *Trans R Soc Trop Med Hyg* 68(3): 258-259.

83. Clyde DF, McCarthy VC, Miller RM & Hornick RB (1973) Specificity of protection of man immunized against sporozoite-induced falciparum malaria. *Am J Med Sci* 266(6): 398-403.

84. RTS, S Clinical Trials Partnership (2015) Efficacy and safety of RTS,S/AS01 malaria vaccine with or without a booster dose in infants and children in africa: Final results of a phase 3, individually randomised, controlled trial. *Lancet* 386(9988): 31-45.

85. Hemler ME (2005) Tetraspanin functions and associated microdomains. *Nat Rev Mol Cell Biol* 6(10): 801-811.

Figures and Tables

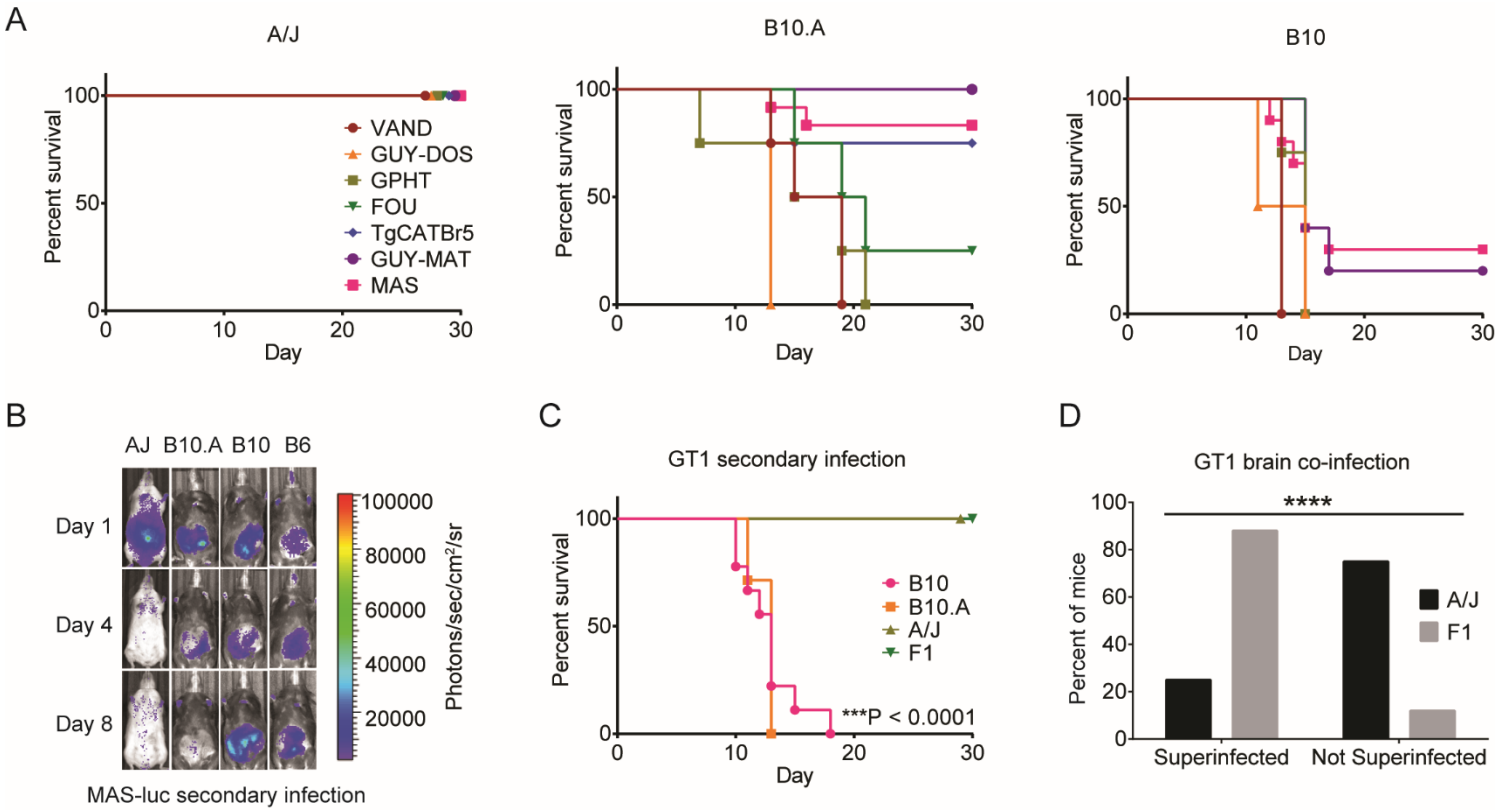

Figure 1. MHC and non-MHC alleles promote immunity to virulent *Toxoplasma gondii* strains in A/J mice.

All mice were primed with 10^4 type III avirulent *T. gondii* CEP *hxgprt-* parasites; then, 35 days later, mice were challenged with $5x10^4$ of the indicated strain of *T. gondii* parasites. A) Survival of A/J [VAND (n=7), GUYDOS (n=5), GPHT (n=5), FOU (n=5), TgCATBr5 (n=5), GUYMAT (n=4), and MAS (n=7)], B10 [VAND (n=4), GUYDOS (n=4), GPHT (n=4), FOU (n=4), TgCATBr5 (n=4), GUYMAT (n=4), and MAS (n=12)], and B10.A [VAND (n=4), GUYDOS (n=4), GPHT (n=4), FOU (n=4), TgCATBr5 (n=4), GUYMAT (n=5), and MAS (n=10)] mice following secondary infection with virulent atypical *T. gondii* strains. Cumulative results are plotted from 1-2 experiments. B) Bioluminescence imaging of individual mice challenged with luciferase expressing MAS strain on days 1, 4 and 8 of

secondary infection; parasite burden is shown as a heat map depicting the relative number of photons (photons/sec/cm2/sr) detected over a 5 minute exposure. C) Survival of B10 (n=5), B10.A (n=5), A/J (n=12), and F1 (A/J x C57BL/6, n=9) mice following secondary infection with the virulent *T. gondii* strain GT1; ***P<0.0001, Log-rank (Mantel-Cox) compared to A/J mice. Cumulative data from 1 to 2 experiments are plotted. D) Superinfection in surviving A/J (n=12) and F1 (A/J x C57BL/6, n=9) following 35 days of secondary infection with the *T. gondii* type I GT1 strain. To evaluate superinfection, brains of A/J (n=12) and F1 (A/J x C57BL/6, n=9) mice were taken from secondary challenge survivors, emulsified, and grown in MPA-xanthine selection medium, which selects for parasites GT1 parasites expressing the endogenous *HXGPRT* locus against the *hxgprt*-type III CEP strain used for chronic infection. The fraction of mice for which the presence of the secondary parasite strain detected (i.e. brain co-infection) or not is plotted; **** P< 0.0001, Fisher's exact test.

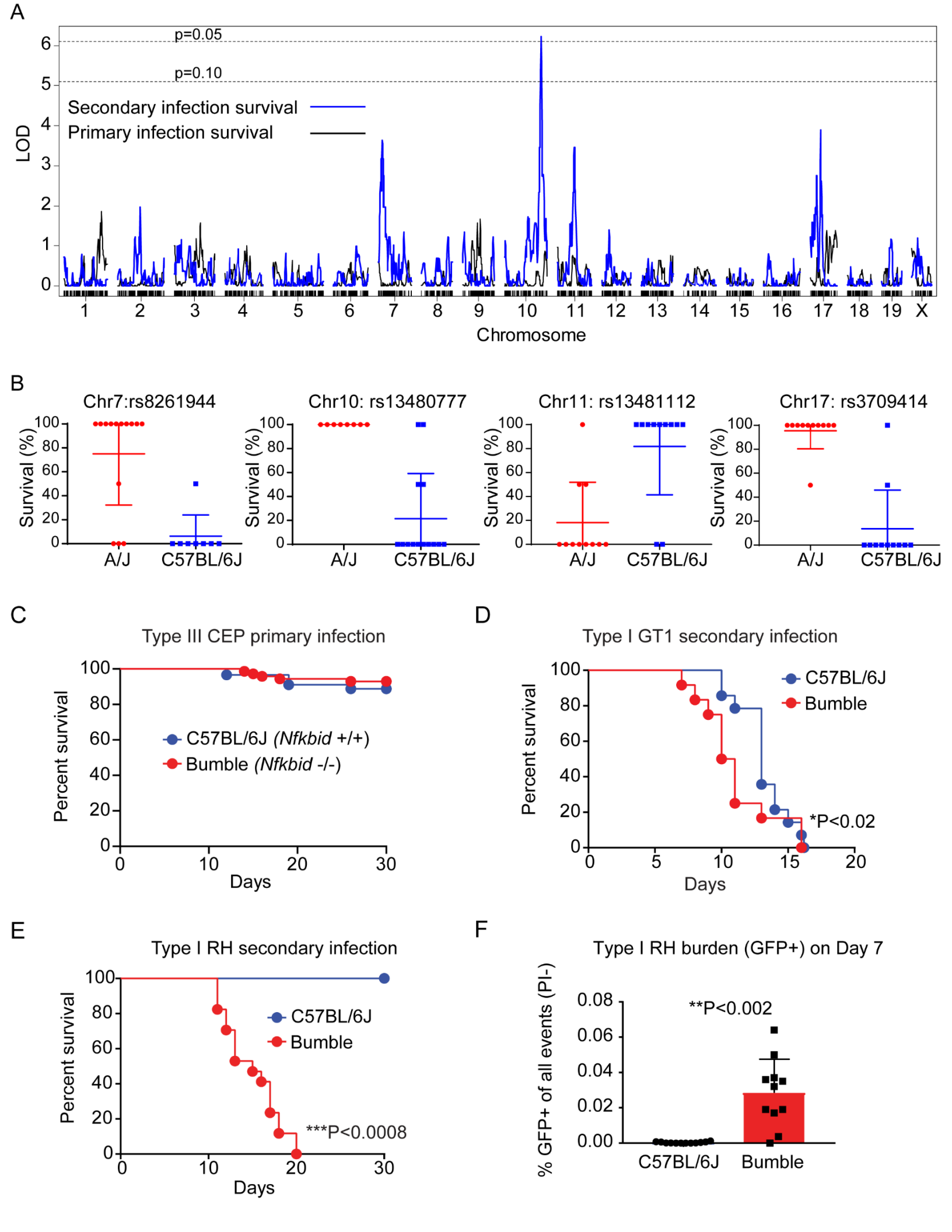
A
p=0.05
p=0.10
Secondary infection survival
Primary infection survival
LOD
Chromosome
B
Chr7:rs8261944
Chr10: rs13480777
Chr11: rs13481112
Chr17: rs3709414
Survival (%)
A/J
C57BL/6J
C
Type III CEP primary infection
Percent survival
C57BL/6J (Nfkbid +/+)
Bumble (Nfkbid -/-)
Days
D
Type I GT1 secondary infection
C57BL/6J
Bumble
*P<0.02
E
Type I RH secondary infection
***P<0.0008
F
Type I RH burden (GFP+) on Day 7
% GFP+ of all events (PI-)
**P<0.002

Figure 2. Genetic mapping reveals *Nfkbid* is required for immunity to *Toxoplasma gondii* secondary infections.

26 recombinant inbred (RI) mouse strains from the AxB;BxA panel were primed with $1x10^4$ type III avirulent *T. gondii* CEP *hxgprt*- parasites; then, 35 days later, mice were challenged with $5x10^4$ virulent type I GT1 *T. gondii* parasites (n=2 per RI line). A) LOD scores for each marker were calculated using Haley-Knott regression and the running LOD scores of primary (black) and secondary infection survival (blue) for each genetic marker is plotted. 1000 permutations were performed to obtain the genome wide threshold LOD values; P=0.10 and 0.05 thresholds are shown. QTL analysis was performed with the program r/QTL (Bowman). B) Effect plots for the genetic markers closest to the maximal LOD scores calculated for the chromosome 7, 10, 11 and 17 QTLs are shown. Each dot indicates the percent survival of a unique RI line and whether it encodes an A/J (red) or C57BL/6 (blue) allele at the specified genetic marker. C) Cumulative survival of bumble (*Nfkbid*-/- C57BL/6) (n=71) and wildtype (C57BL/6J) (n=89) naïve mice infected with the avirulent type III CEP strain. D) Survival of chronically infected bumble (n=12) and wildtype (n=8) mice given a secondary infection with the type I GT1 strain. Cumulative survival from 3 separate experiments are shown; * P<0.02, Gehan-Breslow-Wilcoxon test. E) As in B, but survival to secondary infection with the type I RH strain is shown. Cumulative survival from 3 separate experiments is plotted (bumble n=17, C57BL/6J n=4); ***P<0.008, Mantel-Cox test. F) Frequency of GFP+ events in the peritoneal lavage 7 days post-secondary infection with GFP-expressing type 1 RH strain (RH 1-1). Each dot represents the result of one mouse, and cumulative results are shown from 3 separate experiments (bumble n=13, C57BL/6J n=17); **P<0.002, unpaired two-tailed t-test.

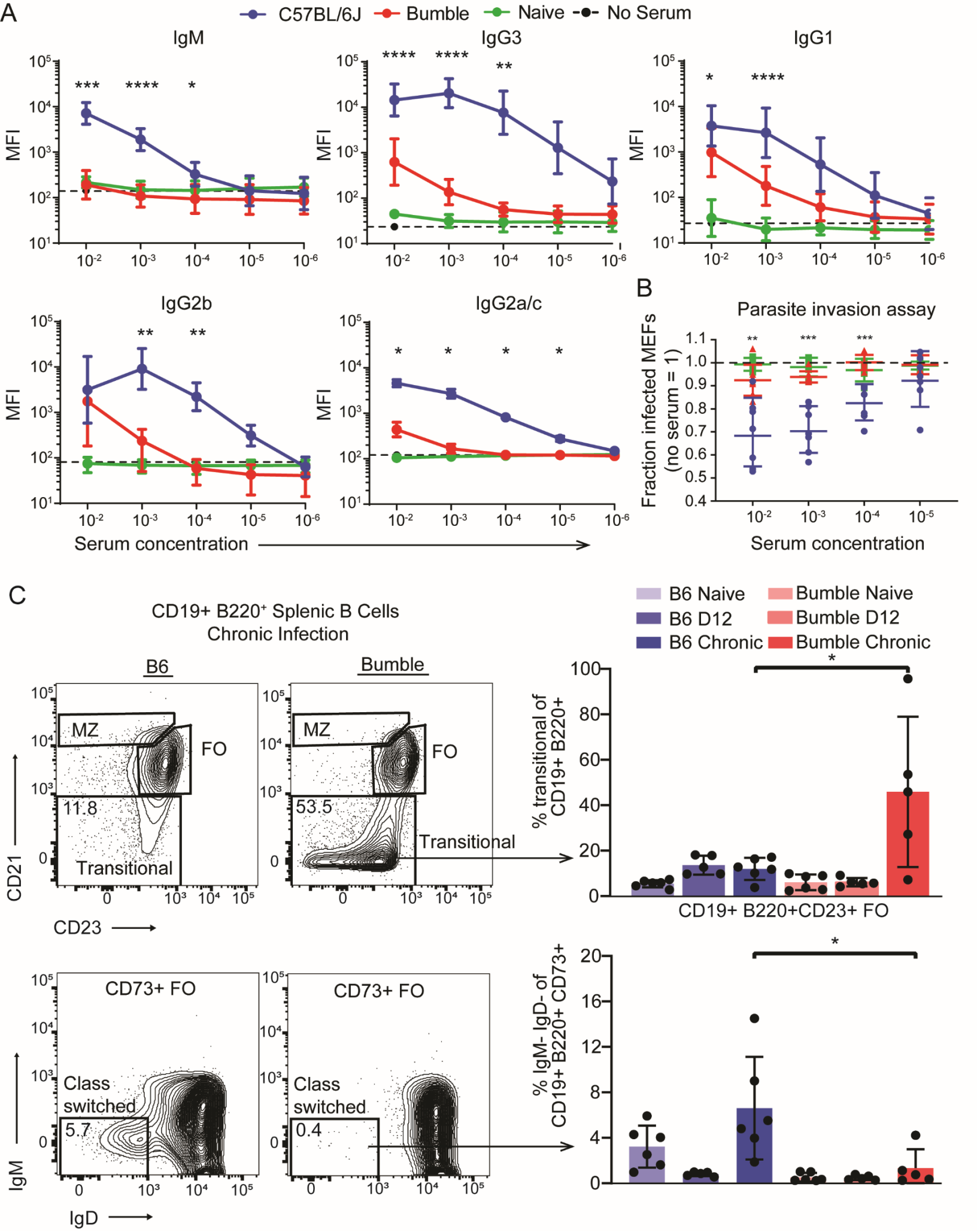
A
C57BL/6J
Bumble
Naive
No Serum
IgM
IgG3
IgG1
IgG2b
IgG2a/c
MFI
Serum concentration
B
Parasite invasion assay
Fraction infected MEFs (no serum = 1)
Serum concentration
C
CD19+ B220+ Splenic B Cells
Chronic Infection
B6
Bumble
MZ
FO
Transitional
11.8
53.5
CD21
CD23
B6 Naive
B6 D12
B6 Chronic
Bumble Naive
Bumble D12
Bumble Chronic
% transitional of CD19+ B220+
CD19+ B220+CD23+ FO
CD73+ FO
Class switched
5.7
0.4
IgM
IgD
% IgM- IgD- of CD19+ B220+ CD73+

Figure 3. *Nfkbid* is required for humoral responses to *Toxoplasma gondii*.

A) Whole fixed GFP+ parasites were incubated with serum from chronically infected mice and stained with fluorescently labeled anti-isotype antibodies and assessed by flow cytometry. Quantification of *T. gondii*-specific antibody isotype binding (IgM, IgG1, IgG2a/c, IgG2b, and IgG3) over a range of serum concentrations is shown. Background staining in the absence of serum is indicated by the dotted line for each isotype. Plotted is the cumulative average +/-SD of the geometric mean fluorescence straining intensity (MFI) from 3 separate experiments (bumble n=8, C57BL/6J n=11). B) Neutralization of GFP+ parasites coated with serum over a range of concentrations from the indicated mice. Parasites were incubated in serum for 20 minutes before infection of mouse embryonic fibroblasts and assessed by FACS 2h later. The fraction of infected host cells (GFP+ cells) is normalized to that of parasite infections without serum. Each dot represents the serum from an individual mouse and cumulative results from 3 separate experiments are shown (bumble n=8, C57BL/6J n=7, naïve n=6). For A and B, significance was assessed by unpaired t-tests with Holm-Sidak correction for multiple comparisons; *** $P< 0.001$, ** $P<0.01$, * $P<0.01$. C) Representative FACS plots of chronically infected bumble and B6 mice and scatter plot of the frequency of splenic B cell compartments quantifying transitional B cells at naïve, d12 of primary infection, and chronic infection. Representative FACS plots of chronically infected bumble and B6 mice and scatter plot of the frequency of IgM- IgD- cells of the CD73+ conventional memory B population. Cumulative data from two experiments n=5-6 mice/condition. * $P<0.05$ by unpaired two-tailed t-test.

A

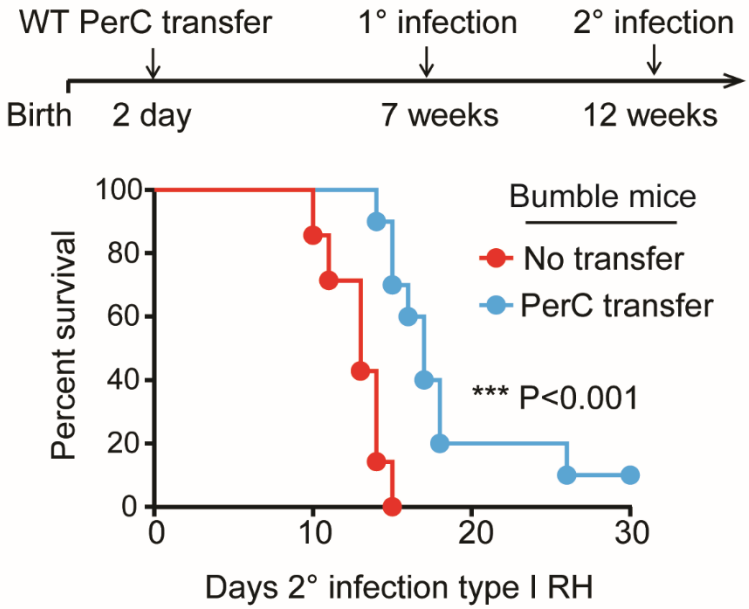

B

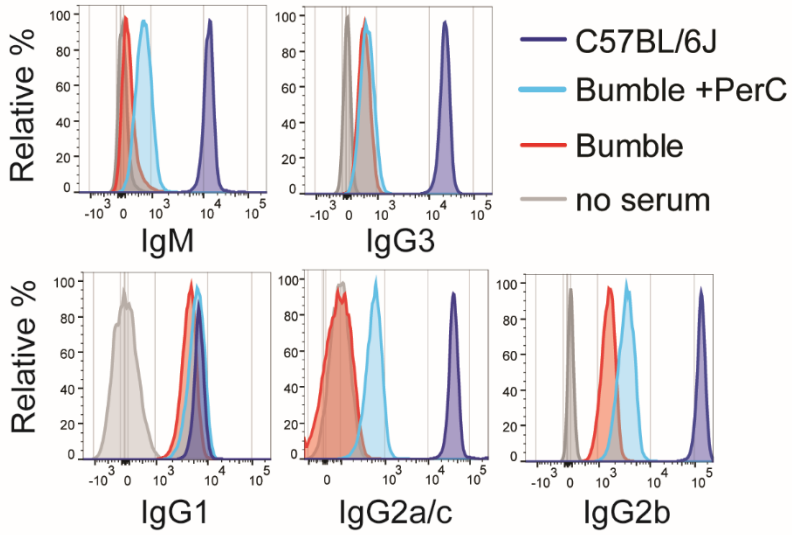

C

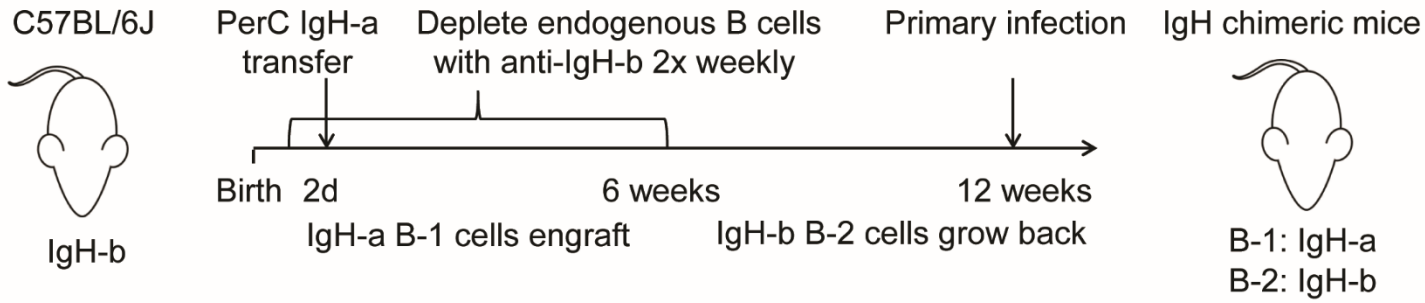

D

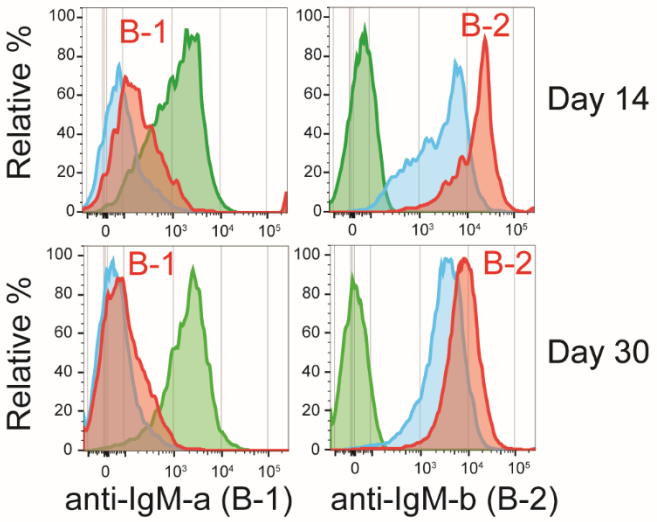

E

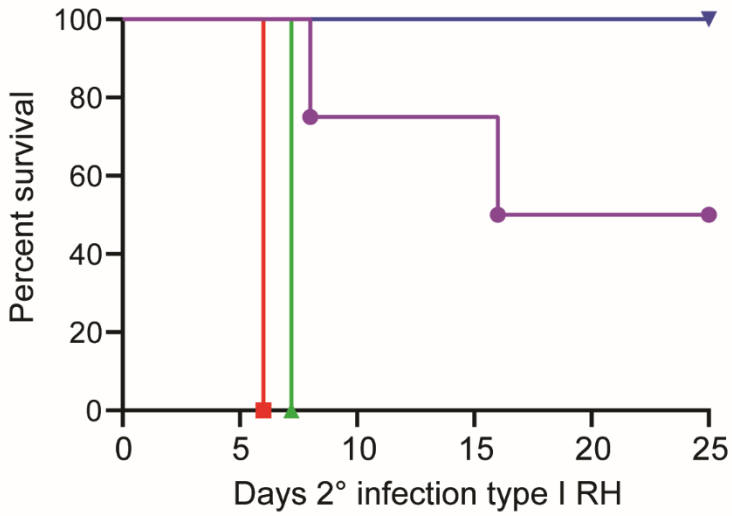

B-1 vs B-2

Infected IgH-a / IgH-b chimeric mice

Staining controls

Infected IgH-b mice

Infected IgH-a mice

Irradiated recipient	BM transfer	PerC transfer
Wt	Wt	Wt
bumble	Wt	Wt
bumble	bumble	Wt
bumble	bumble	-

P<0.05

Figure 4. The contribution of B-1 and B-2 cells to *Toxoplasma gondii* immunity in C57BL/6J mice.

A) Schematic of the secondary infection experiment using PerC reconstituted bumble mice. 2-4 day old bumble neonates were transferred $5x10^6$ total PerC and allowed to rest for 7 weeks before primary infection with type III CEP strain. 5 weeks post-primary infection, mice were given a secondary infection with the type I strain RH. Survival of bumble mice given total PerC transfers (n=10) relative to littermate controls (n=12). Cumulative survival is shown from 3 separate experiments; *** P <0.001, Mantel-Cox test. B) Representative histogram of anti-isotype (IgM, IgG1, IgG3, IgG2a/c, and IgG2b) MFI bound to parasites coated in serum from chronically infected bumble, bumble given PerC transfer, and WT mice. C) Schematic of neonatal allotype chimera generation. C57BL/6J neonates were given anti-IgHb to deplete endogenous B cells at day 1 post birth and twice weekly after for 6 weeks, thereby depleting the endogenous B-1 pool for the life of the animal due to their restricted fetal/neonatal window of development. Neonates were given $5x10^6$ total PerC from 6-8 week old IgH-a congenic C57BL/6 mice donors. These mice then rested for 6 weeks after the last depletion treatment to allow reemergence of the endogenous B-2 IgH-b cells. D) Representative histograms of serum derived anti-IgM-a (B-1 derived) or anti-IgM-b (B-2 derived) staining profiles of type I RH GFP+ parasites taken from the IgH allotype chimeras on day 14 and 30 following primary type III CEP infection. Staining controls with serum from chronically infected C57BL/6J IgH-b littermates, or IgH-a mice are shown. E) Irradiated bumble and WT recipients were given WT or bumble bone marrow (BM) with or without total WTPerC. Mice were vaccinated with a replication deficient type I strain (RH *ΔupΔompdc*) and 30d later challenged with

type I RH. Cumulative survival is shown from 2 experiments (n=6 per condition); * $P<0.05$ by Mantel-Cox test.

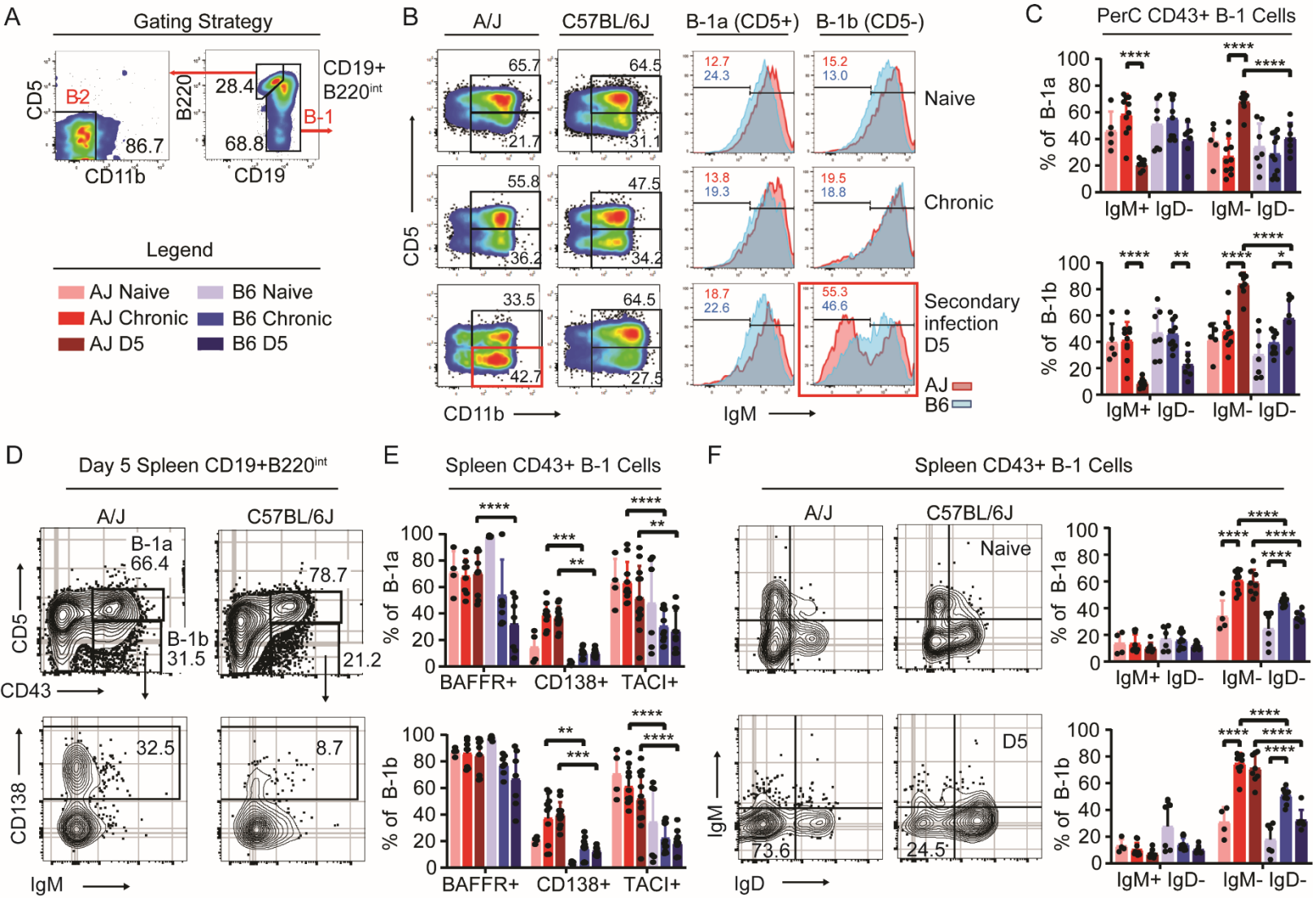

Figure 5. Evidence for enhanced B-1 cell activation in resistant A/J mice.

A) Gating strategies for identifying B-1 B cells. B-1 B cells are identified as CD19+, B220^{int} and CD11b+. B-1a B cells are CD5+ and B-1b B cells are CD5-. The legend applies to panels C-F. B) Representative FACS plots of the peritoneal B-1 B cell compartment (CD19+ B220$^{int\text{-}neg}$ CD11b^{+}) in A/J and C57BL/6J (B6) mice at naïve, chronic, and 5 days (D5) post-secondary infection with the GT1 strain. Numbers indicate the percent of cells that fall within the indicated gate. Representative histograms of IgM surface expression and percent of cells that fall within IgM^{lo} gate of B-1a and B-1b cells from A/J (red) and C57BL/6J (blue) at the indicated time points. Boxed in red highlight the increased frequencies of B-1b B cells that are IgM^{low} on day 5 post-secondary infection with *T. gondii* observed in A/J relative to C57BL/6J mice. C) The frequency of B-1a (CD5+) or B-1b

(CD5-) CD43+ CD19+ B220$^{int-neg}$ B-1 cells from the peritoneum that are IgM+IgD- or IgM+IgD- are indicated. D) Representative FACS plots of splenic CD19+ B220$^{int-neg}$ B cells stained for CD43 and CD5 in A/J and C57BL/6J mice at day 5 of secondary infection. Representative FACS plots of CD138+ cells of CD5- CD43+ CD19+ B220$^{int-neg}$ B-1b B cells . E) Frequencies of CD43+ splenic B-1a and B-1b cells from A/J and C57BL/6J mice that express BAFFR+, TACI+, or CD138+ at the indicated infection states. F) Representative FACS plots and frequencies of splenic B-1a or B-1b (CD19+ B220$^{int-neg}$ CD43+) that are IgM+IgD- or IgM-IgD- in A/J and C57BL/6J mice at the indicated infection states. For C, E and F, the cumulative average +SD from 2-4 experiments are plotted and each dot represents the result from an individual mouse; P values calculated by 2-way ANOVA with Tukey correction; **** P<0.0001, *** P<0.001, ** P<0.01, * P<0.05.

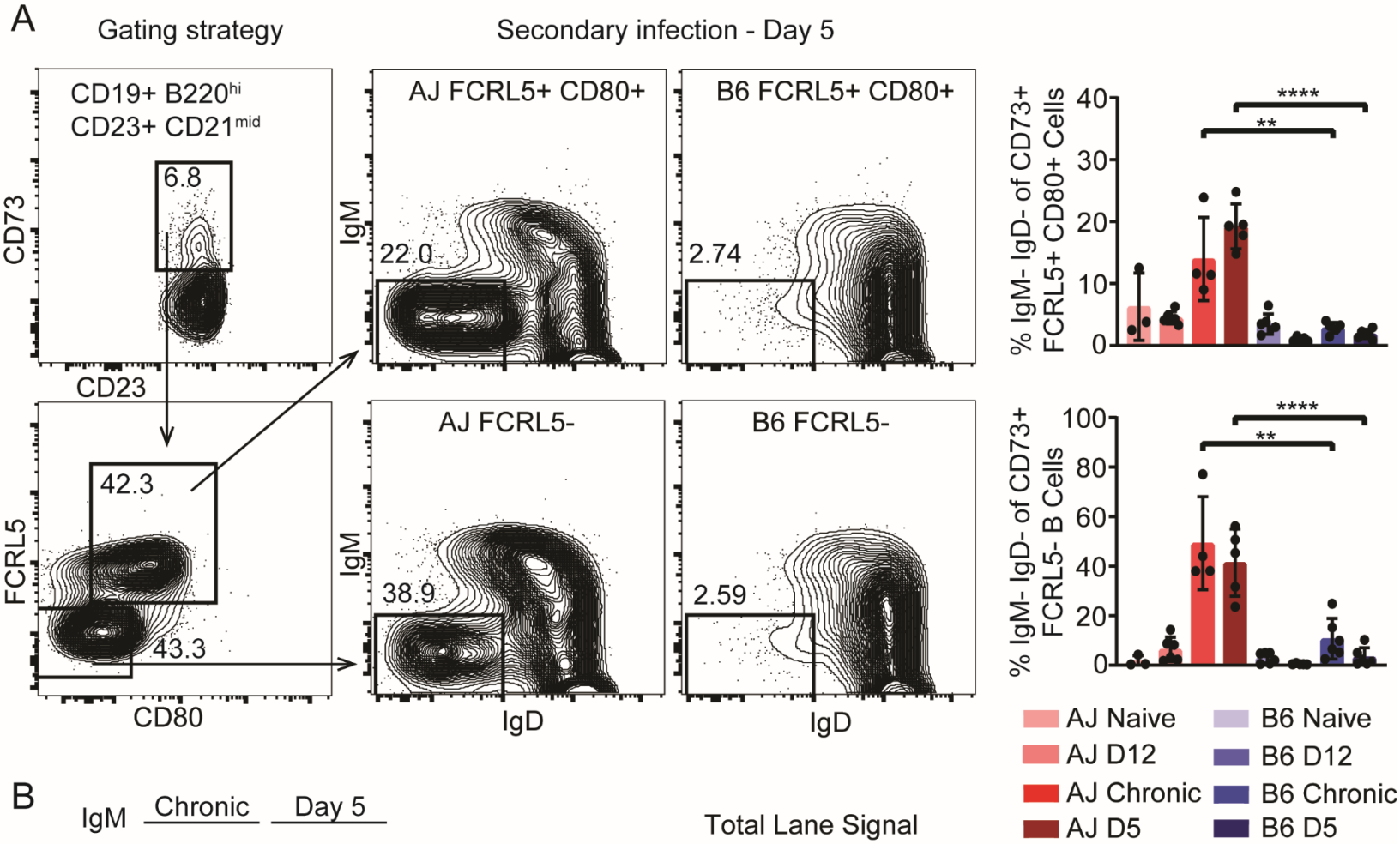
A
Gating strategy
Secondary infection - Day 5
CD19+ B220hi
CD23+ CD21mid
6.8
CD73
CD23
42.3
43.3
FCRL5
CD80
AJ FCRL5+ CD80+
B6 FCRL5+ CD80+
IgM
22.0
2.74
AJ FCRL5-
B6 FCRL5-
38.9
2.59
IgD
% IgM- IgD- of CD73+ FCRL5+ CD80+ Cells
% IgM- IgD- of CD73+ FCRL5- B Cells
****
**
AJ Naive
AJ D12
AJ Chronic
AJ D5
B6 Naive
B6 D12
B6 Chronic
B6 D5

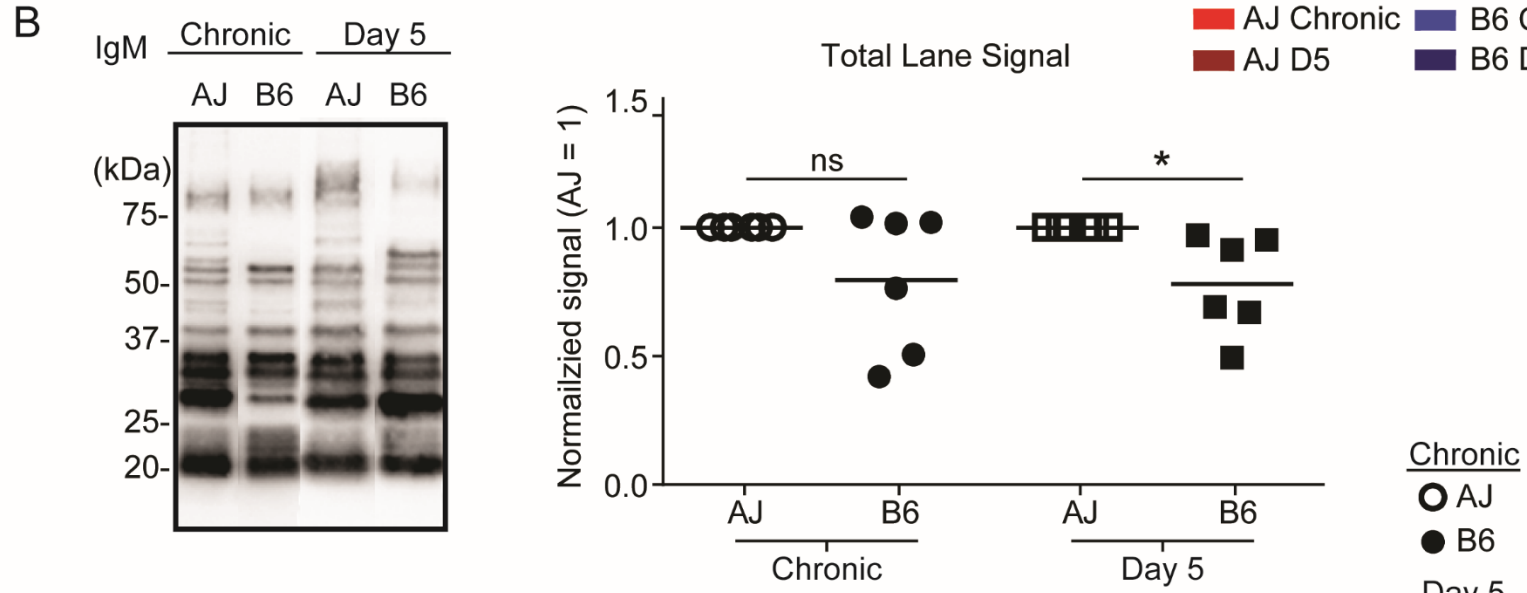
B
IgM
Chronic
Day 5
AJ B6 AJ B6
(kDa)
75-
50-
37-
25-
20-
Total Lane Signal
Normailzied signal (AJ = 1)
ns
*
AJ B6 AJ B6
Chronic
Day 5
Chronic
AJ
B6
Day 5
AJ
B6

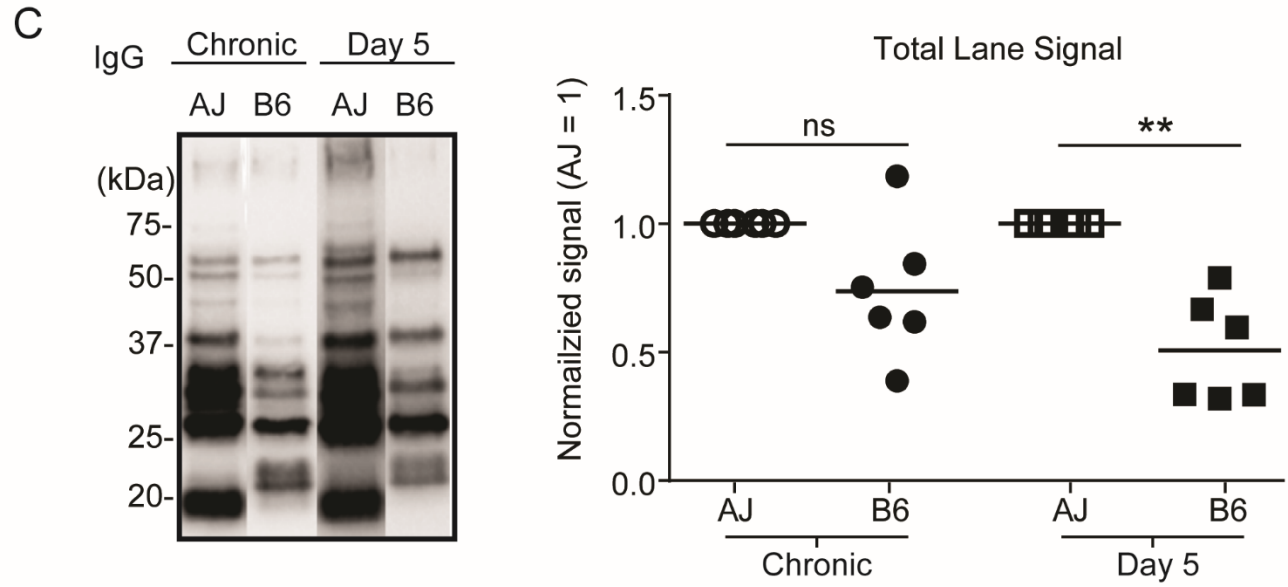
C
IgG
Chronic
Day 5
AJ B6 AJ B6
(kDa)
75-
50-
37-
25-
20-
Total Lane Signal
Normailzied signal (AJ = 1)
ns
**
AJ B6 AJ B6
Chronic
Day 5

Figure 6. Immunity in A/J mice correlates with enhanced class-switching in the memory B cell compartment and increased serum reactivity to parasite lysate antigen.

A) Gating strategies for identifying memory B cells. Memory B cells are identified as CD19+, B220+, CD23+, CD21^{mid}, CD73+. Conventional memory B cells are FCRL5-, CD80-, while atypical memory B cells are identified as FCRL5+, CD80+. Representative FACS plots of memory compartments in A/J and C57BL/6J mice on day 5 of secondary infection with the type I GT1 strain are shown. The frequency of class-switched (IgM-, IgD-) memory cells at the indicated infection states were analyzed. Each dot represents the results from an individual mouse and the cumulative averages +SD from 2 experiments are plotted. N=3-6 mice per infection state. Significance was assessed with an unpaired two-tailed t-test; *** P<0.0001, ** P<0.01. B and C) Western blot analysis of serum-derived antibody reactivity against type I GT1 parasite lysate antigen. Blood plasma was harvested from A/J and C57BL/6J mice either chronically infected with type III CEP *T. gondii* strain, or 5 days post-secondary infection with type I GT1 and used to probe GT1 parasite lysate separated by SDS-PAGE then detected with B) anti-IgM-HRP or C) anti-IgG-HRP. Western blots comparing A/J and C57BL/6J serum reactivity to GT1 lysate were developed and imaged simultaneously to reduce variability in band intensity. Total lane signal is the sum of the colorimetric intensity from lysate bands in a single lane quantified in Image Lab (Bio-Rad). “Total Lane Signal” is normalized lane signal from C57BL/6J compared to A/J which were developed in tandem. Results are from 6 individual experiments; ** P < 0.01, * P < 0.05; unpaired two-tailed t-tests.

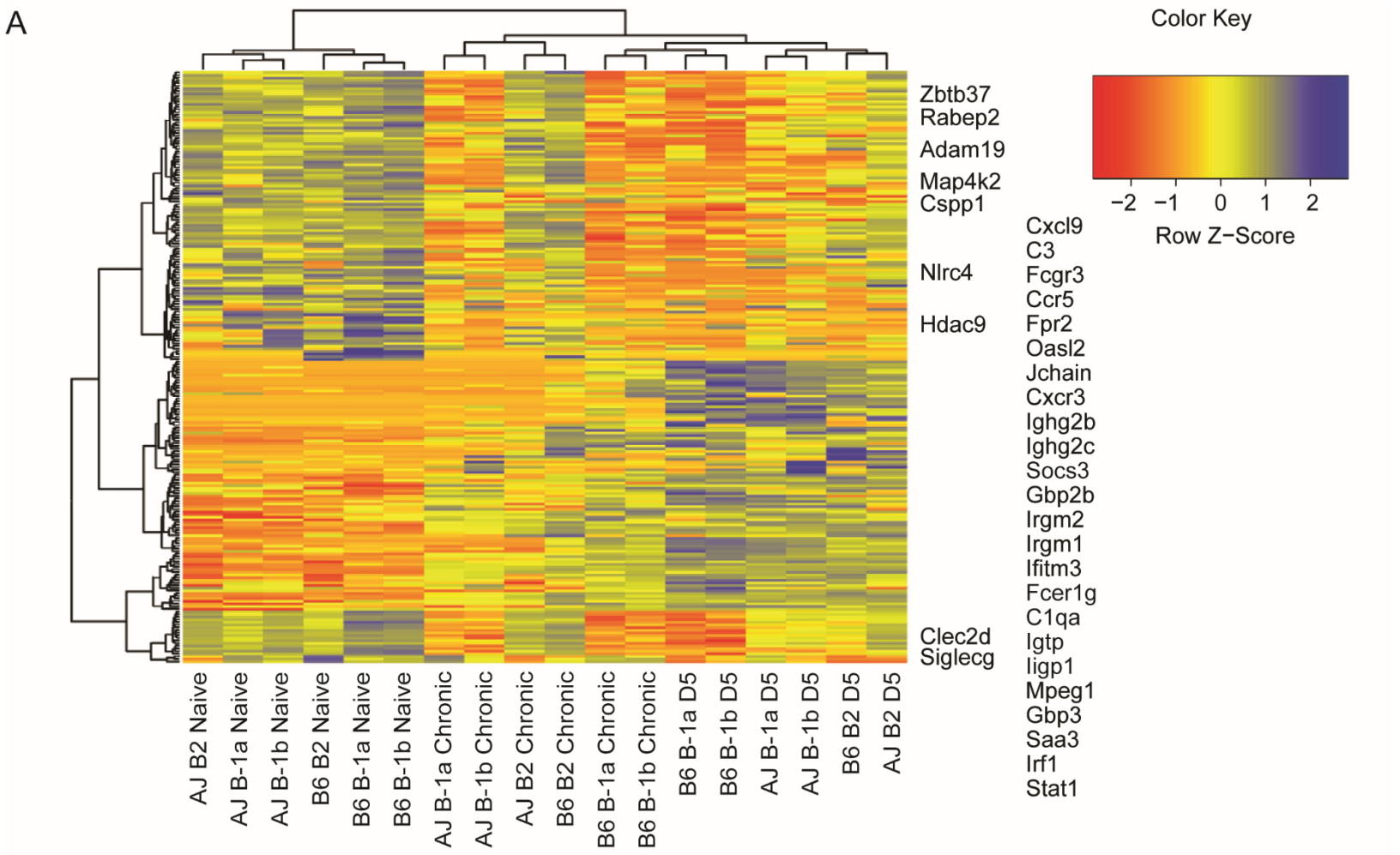

B

Pathway Enrichment	P Value
Immune System	0.00056
Regulation of Complement cascade	0.01682
Innate Immune System	0.02853
Complement cascade	0.03473

GO Term	P Value
defense response	7.27E-19
response to external biotic stimulus	5.09E-15
innate immune response	3.15E-14
response to stress	3.56E-13
response to IFN-γ	8.01E-10
response to IFN-β	8.23E-09
response to bacterium	1.56E-08
inflammatory response	4.40E-07
response to cytokine	8.5E-06
response to protozoan	9.9E-05

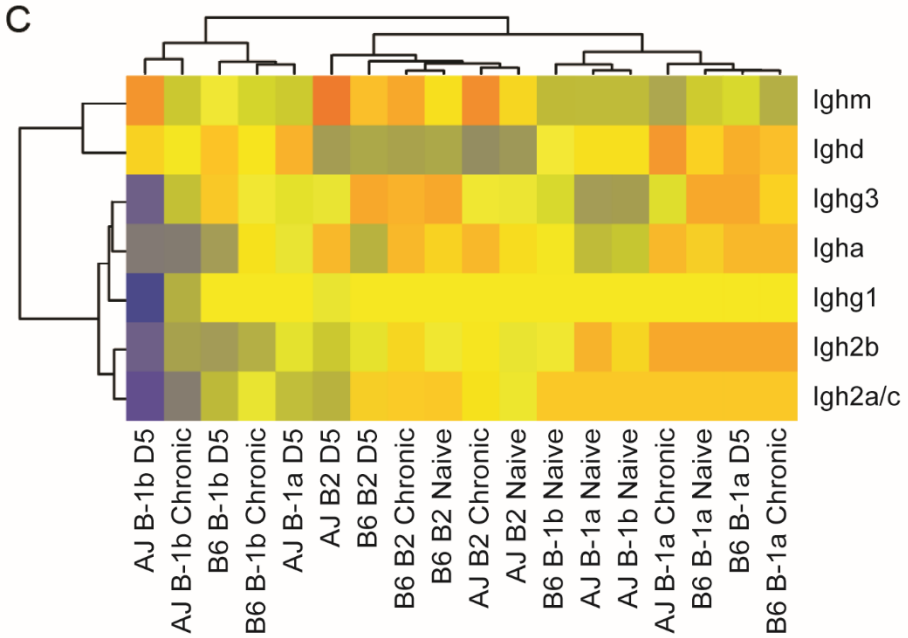

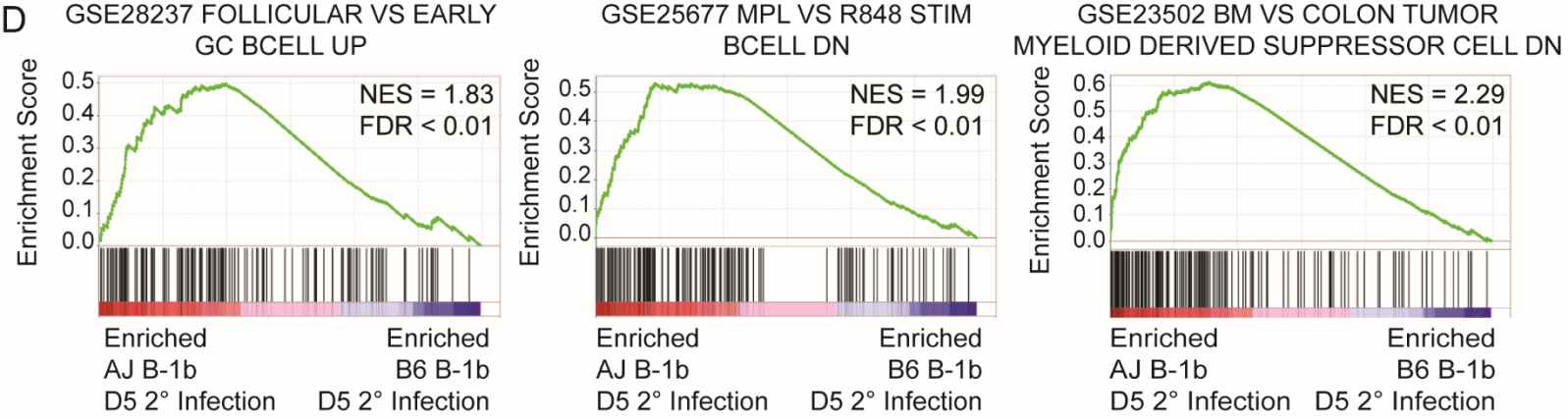

Figure 7. B-1 cells have enhanced germline transcription of *Ighg* constant regions and different activation profiles in resistant A/J mice.

A) Transcriptomic analysis of peritoneal B-1a (CD19+ B220$^{int-neg}$ CD11b+ CD5+), B-1b (CD19+ B220$^{int-neg}$ CD11b+ CD5-) and B-2 (CD19+ B220^{hi} CD11b+ CD5+) B cells from A/J and C57BL/6J mice, that were either naïve, chronically infected, or on day 5 of secondary infection with the type I GT1 strain, was performed using 3'-Tag RNA sequencing. The heat map depicts the relative expression of genes that were: i) at least fourfold differentially expressed in any of the B cell compartments when comparing its expression between the naïve and either chronic or secondary infection states; and ii) it made the cutoff in at least three separate comparisons irrespective of genetic background. B) Pathway and GO term enrichment of the genes depicted in A; P values were calculated with Holm-Bonferroni adjustments. C) Heatmap depicting the relative expression of all *Ighg* transcripts from the indicated B cell population, mouse strain and infection state. D) Gene set enrichment analysis of the rank-ordered list of differentially expressed genes between A/J and C57BL/6J B-1b cells at day 5 of secondary infection. Gene sets depicted (GSE28237, GSE25677 and GSE23502) were in the top 10 gene sets ranked by false discovery rate (FDR) after investigating MSigDB's C7: immunologic signatures collection. Enrichment score is the degree of overrepresentation of a gene set at the top or bottom of a ranked list. NES is the enrichment score after normalizing for gene set size.

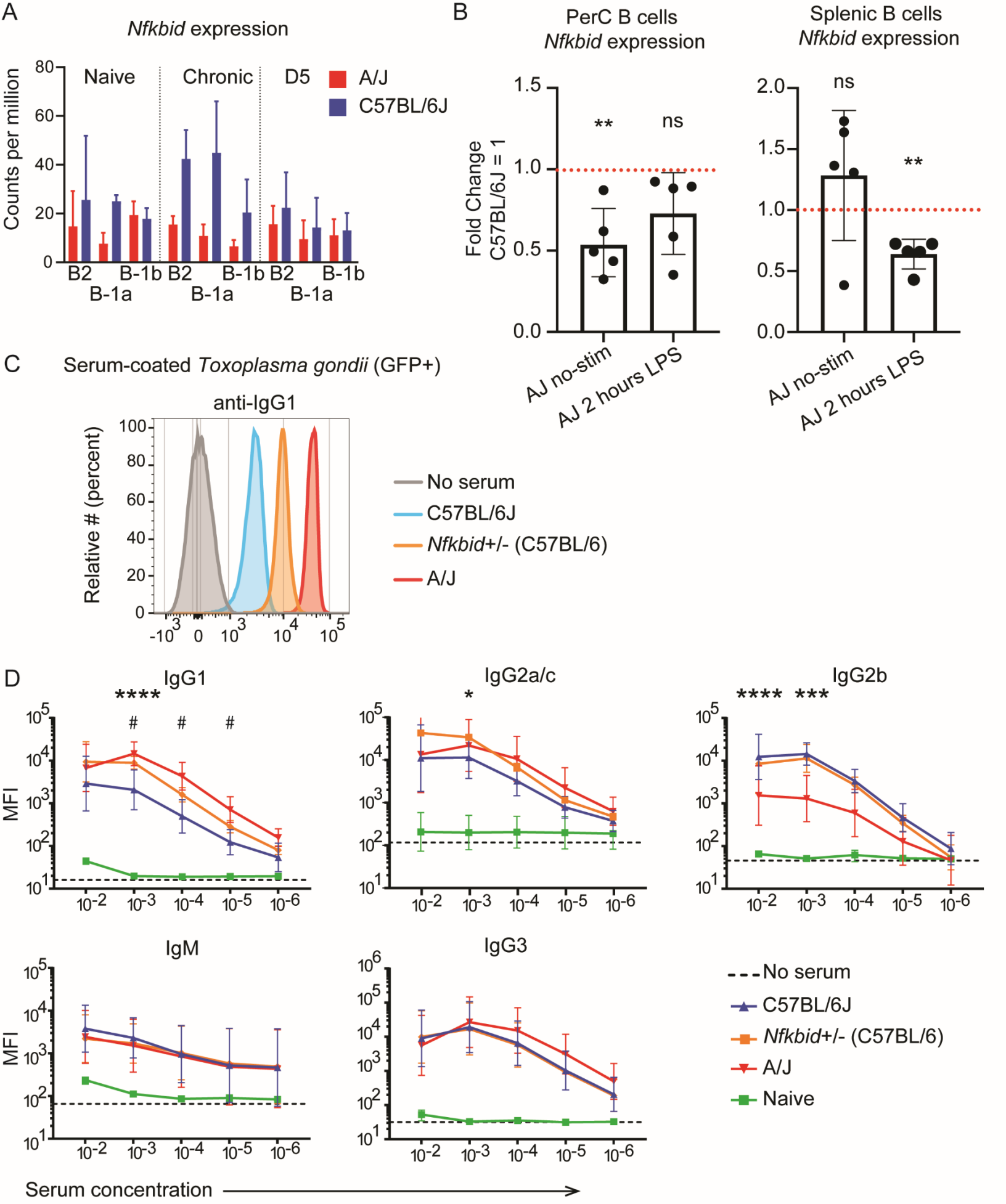
A
Nfkbid expression
Counts per million
Naive
Chronic
D5
A/J
C57BL/6J
B2
B-1b
B-1a
B
PerC B cells
Nfkbid expression
Splenic B cells
Nfkbid expression
Fold Change
C57BL/6J = 1
**
ns
AJ no-stim
AJ 2 hours LPS
C
Serum-coated Toxoplasma gondii (GFP+)
anti-IgG1
Relative # (percent)
No serum
C57BL/6J
Nfkbid+/- (C57BL/6)
A/J
D
IgG1
IgG2a/c
IgG2b
IgM
IgG3
MFI
****
***
*
#
No serum
C57BL/6J
Nfkbid+/- (C57BL/6)
A/J
Naive
Serum concentration

Figure 8. Gene dosage of *Nfkbid* impacts parasite-specific IgG1 responses.

A) *Nfkbid* expression in CPM (Counts per million) of 3'-Tag RNA-seq reads of the indicated B cell populations obtained from A/J and C57BL/6J mice that were either naïve, chronically infected, or on day 5 of secondary infection with the type I GT1 strain. B) Enriched B cells from the PerC and spleen were stimulated with LPS for 2 hrs and *Nfkbid* transcripts were quantified by qPCR; ** P< 0.01, paired t-test. C) Representative histograms display the detection of parasite-specific IgG1 bound to formaldehyde fixed GFP+ type I GT1 parasites; diluted serums (10^3) from C57BL/6J, *Nfkbid*+/- (C57BL/6J x bumble F1), and A/J mice chronically infected with the type III CEP strain were assayed. Anti-mouse IgG1 background staining in the absence of serum is shown. D) As in C, but quantification of the parasite-specific antibody isotype binding (IgM, IgG1, IgG2a/c, IgG2b, and IgG3) over a range of serum concentrations is shown. Background staining in the absence of serum is indicated for each isotype. Plotted is the cumulative average +/-SD of the geometric mean fluorescence straining intensity (MFI) from 2-3 separate experiments (C57BL/6J n=8; *Nfkbid*+/- n=7; A/J n=8); significance was assessed by unpaired t-tests and Holm-Sidak corrections comparing A/J vs C57BL/6J (*) or *Nfkbid+/-* vs C57BL/6J (#); **** P< 0.0001, *** P< 0.001, */# P<0.05. IgG1 staining was not significantly different between A/J and *Nfkbid*+/- serums.